Climate Dynamics (2021) 56:3775–3795
https://doi.org/10.1007/s00382-021-05666-3

Coupling ocean–atmosphere intensity determines ocean chlorophyll-induced SST change in the tropical Pacific

Feng Tian[1,2,3] · **Rong-Hua Zhang**[1,2,3,4] · **Xiujun Wang**[5]

Received: 22 July 2020 / Accepted: 19 January 2021 / Published online: 6 February 2021

Abstract

Phytoplankton pigments (e.g., chlorophyll-a) absorb solar radiation in the upper ocean and induce a pronounced radiant heating effect (chlorophyll effect) on the climate. However, the ocean chlorophyll-induced heating effect on the mean climate state in the tropical Pacific has not been understood well. Here, a hybrid coupled model (HCM) of the atmosphere, ocean physics and biogeochemistry is used to investigate the chlorophyll effect on sea surface temperature (SST) in the eastern equatorial Pacific; a tunable coefficient, α, is introduced to represent the coupling intensity between the atmosphere and ocean in the HCM. The modeling results show that the chlorophyll effect on the mean-state SST is sensitively dependent on α (the coupling intensity). At weakly represented coupling intensity ($0 \le \alpha < 1.01$), the chlorophyll effect tends to induce an SST cooling in the eastern equatorial Pacific, whereas an SST warming emerges at the strongly represented coupling intensity ($\alpha \ge 1.01$). Thus, a threshold exists for the coupling intensity (about $\alpha = 1.01$) at which the sign of SST responses can change. Mechanisms and processes are illustrated to understand the different SST responses. In the weak coupling cases, indirect dynamical cooling processes (the adjustment of ocean circulation, enhanced vertical mixing, and upwelling) tend to dominate the SST cooling. In the strong coupling cases, the persistent warming induced by chlorophyll in the southern subtropical Pacific tends to induce cross-equatorial northerly winds, which shifts to anomalous westerly winds in the eastern equatorial Pacific, consequently reducing the evaporative cooling and weakening indirect dynamical cooling; eventually, SST warming maintains in the eastern equatorial Pacific. These results provide new insights into the biogeochemical feedback on the climate and bio-physical interactions in the tropical Pacific.

1 Introduction

The variations of sea surface temperature (SST) in the tropical Pacific strongly influence the global climate change (Kosaka and Xie 2013; England et al. 2014; Forget and Ferreira 2019). Yet there exist large, systematic biases in simulated SST fields in the tropical Pacific as indicated in the state-of-the-art climate models participating in the Coupled Model Intercomparison Project phase 5 (CMIP5) and more recently in CMIP6 (e.g., Wang et al. 2014; Zhu et al. 2020), including an excessive westward extension of the cold tongue. These systematic biases can significantly affect future climate projection (Li et al., 2016; Seager et al. 2019). Large efforts have been made to improve the SST simulations in the tropical Pacific, through modifying the vertical mixing parameterization (e.g., Zhu and Zhang 2018, 2019), air–sea coupling processes (Luo et al. 2005), the effect of the Galápagos Islands (Karnauskas et al. 2007), and so on. In addition, ocean chlorophyll-induced SST change is shown to contribute to improvement of the annual mean

✉ Rong-Hua Zhang
rzhang@qdio.ac.cn

1 Key Laboratory of Ocean Circulation and Waves, Institute of Oceanology, and Center for Ocean Mega-Science, Chinese Academy of Sciences, Qingdao 266071, China

2 Laboratory for Ocean and Climate Dynamics, Pilot National Laboratory for Marine Science and Technology, Qingdao 266237, China

3 University of Chinese Academy of Sciences, Beijing 10029, China

4 Center for Excellence in Quaternary Science and Global Change, Chinese Academy of Sciences, Xi'an 710061, China

5 College of Global Change and Earth System Science, Beijing Normal University, and Joint Center for Global Change Studies, Beijing 100875, China

SST simulation in the tropical Pacific (e.g. Murtugudde et al. 2002; Lim et al. 2018).

Ocean chlorophyll absorbs downwelling shortwave radiation penetrating the sea surface, which alters the vertical distribution of radiant heating in the upper ocean, consequently affecting the heat budget in the mixed layer (Paulson and Simpson 1977; Lewis et al. 1990; Morel and Antoine 1994; Siegel et al. 1995; Ohlmann et al. 2000). In the equatorial Pacific, however, the influence of chlorophyll on annual mean SST is still subject to debate, i.e. whether chlorophyll induces a cooling or warming effect on SST in the ocean and coupled ocean–atmosphere models. In terms of the cooling effect, the processes are involved as follows. Chlorophyll acts to absorb more solar radiation within the mixed layer and further enhances oceanic stratification. The shoaling of the mixed layer (ML) can lead to a stronger Ekman divergence (e.g. Sweeney et al. 2005; Park et al. 2014a, b; Lim et al. 2018; Löptien et al. 2009; Gnanadesikan and Anderson 2009), which generates anomalous westward geostrophic currents north and south of the equator (Nakamoto et al. 2001; Lin et al. 2007, 2008, 2011; Löptien et al. 2009). These processes induce a stronger upwelling, which further induces the upper ocean cooling. The cold SST anomalies induced by the presence of chlorophyll can be further amplified through large-scale ocean–atmosphere interaction (e.g. Park et al. 2014a; Lim et al. 2018), i.e. Bjerknes feedback (Bjerknes 1969). In terms of the warming effect, on the other hand, the vertical distribution of chlorophyll (e.g., deep chlorophyll maximum, DCM) acts to trap more solar radiation in the subsurface and leads to a subsurface warming, which tends to trigger a deepening of the ML and results in a weakening of the westward surface currents; consequently inducing a warming effect in the eastern equatorial Pacific (Murtugudde et al. 2002; Marzeion et al. 2005). Lengaigne et al. (2007) also found that the direct heating in the upper ocean induced by chlorophyll tends to suppress the indirectly dynamical cooling that arises from the change in meridional circulation cell as suggested above, eventually leading to an SST warming in the eastern equatorial Pacific.

The controversial effects on the SST (warming or cooling) in the eastern tropical Pacific presented above are partially attributed to the way to represent chlorophyll effects in the model, the differences in the configuration of control simulations, and differences in representing coupling processes between the ocean and atmosphere with various models adopted. Some discussions of these factors can be expressed as follow. (1) In terms of the way to represent the chlorophyll effects in the model, through imposing spatially variable chlorophyll from ocean color remote sensors on the ocean general circulation model (OGCM), the experiments for chlorophyll-induced effects on the tropical Pacific climate have been widely performed (Nakamoto et al. 2001; Anderson et al. 2007, 2009; Lin et al. 2007, 2008, 2011; Ballabrera-Poy et al. 2007; Gnanadesikan and Anderson 2009). Also, the Earth System Models (ESMs) including ocean biogeochemical components are utilized to study the interactive effect between the chlorophyll and climate, with focusing on the change in mean-state SST and ENSO (Wetzel et al. 2006; Lengaigne et al. 2007; Löptien et al. 2009; Jochum et al. 2010; Patara et al. 2012; Park et al. 2014b, a; Lim et al. 2018). (2) To isolate the net effects of spatially varying or interactively varying chlorophyll, the penetration depth of solar radiation in the ocean (H_p) is set to be varying from 11 to 43 m in the control experiments (e.g., Wetzel et al. 2006; Gnanadesikan and Anderson 2009). Thus, the resultant effects are only qualitatively comparable with each other. (3) Not only the control simulation design is various, but also the model adopted is different. For example, the earlier studies tend to utilize OGCM without considering atmospheric feedback to investigate the effect of chlorophyll on the ocean (Nakamoto et al. 2001; Murtugudde et al. 2002; Sweeney et al. 2005; Löptien et al. 2009). When the coupled climate models are introduced to examine this effect, the chlorophyll-induced SST change in the eastern equatorial Pacific also exhibits diverse response under different coupling intensity, i.e., SST warming (e.g., Lengaigne et al. 2007; Patara et al. 2012) or cooling (e.g., Gnanadesikan and Anderson 2009; Park et al. 2014a).

Although previous studies have examined the effects of chlorophyll on the ocean (e.g., ocean dynamical processes), the roles of the atmosphere or ocean–atmosphere interaction in the effect of chlorophyll have not been investigated well. Ocean chlorophyll-induced local SST change can be amplified or damped through the coupling between the ocean and atmosphere (Gildor 2003; Shell 2003; Liang and Wu 2013). Currently, the way to represent coupling intensity can be varying among different coupled models due to the differences in the parameterizations of the atmospheric boundary layer, convective processes, or coupling technique (Guilyardi 2006; Bellenger et al. 2014). Physically, the coupling intensity indicates how strongly the atmospheric wind stress responds to the SST anomalies (Guilyardi 2006). The coupling intensity is considered to be relatively constant in each model without considering the contributions from internal variability and external forcing. According to the estimation of coupling intensity (regression of Niño4 wind stress over Niño3 SST, or positive Bjerknes feedback) from Bellenger et al. (2014), most models underestimate the coupling intensity by 20–50%, and the intermodel spread for coupling intensity is also huge. Consequently, the large intermodel differences in coupling intensity may further modify the surface warming initially induced by chlorophyll in the eastern equatorial Pacific, and subsequently change the ocean–atmosphere coupling process like Bjerknes feedback (Bjerknes 1969) and wind-evaporation-SST (WES) feedback (Xie and Philander 1994). Furthermore, the differences in

coupling intensity may hinder the intercomparison of results among climate models in terms of chlorophyll-induced SST change in the tropical Pacific.

To figure out the impact of chlorophyll on the tropical Pacific SST under the ocean–atmosphere coupling condition and identify the sensitivity of this impact to the varying coupling intensity, a series of experiments are performed using a hybrid coupled model of the atmosphere, ocean physics and biogeochemistry (HCM-AOPB) (Zhang et al. 2020). In this HCM-AOPB, the coupling intensity can be explicitly tunable through a coefficient (α), which is not explicitly attainable in the current fully coupled climate models. By adjusting it, we can illustrate the potential influence of the coupling intensity between ocean and atmosphere on the SST change in the presence of chlorophyll-induced effect. We are particularly interested in whether there exists a threshold for coupling intensity at which SST states can make transition from a cooling (warming) condition to a warming (cooling) condition in the presence of the chlorophyll effect. Then, we try to understand which physical processes (indirect dynamical or direct thermodynamical processes) are responsible for determining such transitions between warming and cooling. Note that on the physical side, the role of coupling ocean–atmosphere intensity in modulating SST of the tropical Pacific has been intensively investigated (Zhang et al. 2013; Gao and Zhang 2017), but on the ocean biological side, it has not been clearly demonstrated.

The paper is organized as follows. Section 2 is concerned with the model description, data source, and experimental design. Section 3 describes the results for the effect of chlorophyll-induced SST change under two extreme cases (uncoupled ($\alpha = 0.0$) and strongly coupled ($\alpha = 1.15$)), with the related mechanisms being investigated in detail; a series of experiments with gradually increasing coupling intensities were performed, in which a threshold for the coupling intensities is found, at which the effect of chlorophyll-induced change on the SST in the eastern equatorial Pacific can reverse from cooling to warming, and the characteristic of SST evolution due to chlorophyll effect is clearly identified. Section 4 presents a conclusion and discussion.

2 Model, experiments, and data used

2.1 Model description

The numerical experiments are performed using a hybrid coupled model (HCM), which consists of the atmosphere, ocean physics, and biogeochemistry (AOPB). A brief description is presented in the following section and a detailed description can be found in Zhang et al. (2018a, 2020).

2.1.1 An ocean general circulation model (OGCM)

The OGCM used is a reduced-gravity, primitive equation, and sigma coordinate model, specially developed for the tropical ocean (Gent and Cane 1989). The model domain covers the entire tropical Pacific (120º E–76º W, 30º S–30º N). The horizontal resolution is 0.3º–0.6º near the equator. The model has 20 vertical layers, with an explicit bulk mixed layer in the uppermost layer (Chen et al. 1994); mixed layer depth (MLD) is determined by a hybrid vertical mixing scheme, which consists of three major mechanisms of vertical turbulent mixing (wind stirring, shear instability, and convective overturning) (Kraus and Turner 1967; Price et al. 1986). An advective atmosphere mixed layer model (AML) is embedded into the ocean model to determine the sea surface heat flux (Seager et al. 1995; Murtugudde et al. 1996). Within the AML model, air temperature and humidity are determined by several factors such as the surface heat fluxes, horizontal advection induced by winds, entrainment from above the mixed layer, horizontal diffusion, and radiative cooling. Thus, atmospheric advection and eddy transports are considered to alter the relative humidity, which further affects the SST (Murtugudde et al. 1996).

2.1.2 A hybrid coupled ocean–atmosphere model

A statistical atmospheric model is used to determine interannual anomalies of wind stress (Syu et al. 1995; Chang et al. 2001; Zhang and Busalacchi 2009). The coupling between the OGCM and the statistical atmosphere model forms a hybrid-coupled model (HCM; Zhang et al. 2020). Within the HCM context, the total wind stress is separated into a climatological part (τ_{clim}) and an interannual anomaly part (τ_{inter}): $\tau = \tau_{clim} + \tau_{inter}$. τ_{inter} is determined by interannual anomalies of SST (SST_{inter}) according to its empirical model, i.e. $\tau_{inter} = \alpha \bullet F(SST_{inter})$. Note that α is a dimensionless quantity, which is introduced to represent the coupling intensity between SST and wind stress at large scale, and $F(SST_{inter})$ is constructed from a singular value decomposition (SVD) analysis derived from the historical data (Zhang et al. 2005). Because interannual wind responses to SST anomalies are sensitively dependent on seasonality during the ENSO cycle, the seasonality of the wind response to SST anomalies has been taken into account through separately performing the SVD analyses for each calendar month (Zhang et al. 2019a, b). Next, interannual wind stress anomalies (τ_{inter}) are added onto τ_{clim} to force the ocean model at each model step to represent atmospheric wind stress effect on the ocean. It is noted that, in this hybrid coupled model, coupling intensity only refers to the coupling between wind stress and SST,

and other negative feedbacks from like shortwave feedback are not considered into this model, which are included in the state-of-the-art coupled climate model.

Testing indicates that using $\alpha = 1.15$ leads to HCM simulations that have reasonable interannual SST variations, with a quasi-4-year oscillation. The coupled model is then integrated for 100 years and continually integrated forward (Zhang et al. 2018a).

2.1.3 Coupling between the ocean physics and biogeochemistry

Furthermore, the atmosphere–ocean coupled model is combined with an ocean biogeochemical model (Christian et al. 2001; Wang et al. 2008), which consists of 12 components (e.g. nitrate, iron, phytoplankton, zooplankton, and so on). Chlorophyll is estimated using a ratio between phytoplankton biomass and chlorophyll, called the C: Chl ratio (Wang et al. 2009a). More details can be found in previous studies (Zhang et al. 2018b; Tian et al. 2018). Then, chlorophyll is introduced into a bio-optical model to represent its effect on the penetrative solar radiation (Wang et al. 2009a). This bio-optical model is calculated as follows:

$$K_A(k) = K_w + K_C Chl(k) \quad (1)$$

where K_A is the total attenuation coefficient for shortwave radiation, $K_W = 0.028\ \mathrm{m}^{-1}$ is the seawater attenuation coefficient, $K_C = 0.058\ \mathrm{m}^{-1}\ (\mathrm{mg\ m}^{-3})^{-1}$ is the attenuation coefficient for chlorophyll. *Chl (k)* is the concentration for chlorophyll at each model layer; *k* denotes the number of the model layer. Next, the reciprocal of K_A denotes the penetration depth (H_p), which is embedded into the ocean general circulation model to parameterize the effect of chlorophyll on the penetrative solar radiation.

2.2 Experimental design and data used

We perform two types of experiments to separate the effect of chlorophyll on the mean state in the tropical Pacific. In a control simulation (a case to treat the ocean as pure water), named PURE, the biogeochemical model is not activated in the HCM and the chlorophyll concentration is set to zero everywhere; thus, the chlorophyll-induced effect on SST is not considered in the model. In the second simulation, named CHL, the biogeochemical model is activated in the model and the simulated chlorophyll can directly affect the penetration of solar radiation in the ocean. Differences between CHL and PURE are used to represent the effect of total chlorophyll on the ocean. This experimental design has been widely adopted to examine the total effect of chlorophyll on the climate under the condition with the uncoupled (ocean-only) models or coupled models (Gnanadesikan and Anderson 2009; Park et al. 2014a, b). Previously, interannually and intraseasonally varying (e.g., tropical instability waves) chlorophyll effects have been demonstrated to produce a substantial change in the mean state and variability of the tropical Pacific climate (Zhang et al. 2009; Tian et al. 2018, 2019); these multi-scale chlorophyll effects on the tropical Pacific climate are included in this modelling study as a whole.

We perform a series of experiments using HCM, in which different coupling intensities can be explicitly adjustable, ranging from uncoupled ($\alpha = 0.0$) to coupled ($\alpha > 0.0$) conditions; it is quite difficult to perform such experiments using current fully coupled models. The coupling intensities (α) are set to be 0.0, 0.5, 0.8, 1.0, 1.1, and 1.15 to represent different intensities of the ocean–atmosphere coupling. The case with $\alpha = 0.0$ represents an ocean-only case, without any large-scale feedback from the atmosphere. It is noted that different from the traditional ocean-only simulation with prescribed surface heat fluxes (ocean-only case), a non-local atmospheric mixed-layer parameterization, as described in the previous section, is introduced into the HCM to reasonably simulate seasonal SST variability (Murtugudde et al. 1996). Therefore, the case with $\alpha = 0.0$ would not mean that the HCM is a pure ocean-only model. The case with $\alpha = 1.15$ represents a strong coupling with atmospheric wind feedback onto the ocean, and its ENSO amplitude (measured by the standard deviation of Niño3.4 SST anomalies) is 1.03℃, which is larger than that in the observation (≈ 0.87 ℃). By performing these experiments, the effects of chlorophyll on SST in the eastern tropical Pacific can be illustrated; a striking feature emerges: the mean-state SST conditions in the eastern equatorial Pacific can be reversed from cooling to warming when α is taken from $\alpha = 1.0$ to 1.1. To understand more details of the effects, we further perform experiments with α intervals being set to 0.01 from 1.0 to 1.1, so that the potential threshold can be detected. The model is integrated for 60 years in all experiments, and the results from the last 40 years of each run are used for analyses.

The observed sea surface chlorophyll data from the GlobColour project during the period of 1998–2016 are used to validate the simulation (Fig. 1a and c) (Maritorena et al. 2010). The observed chlorophyll data with the original grid being 0.25° × 0.25° are binned into the model grid.

3 Results

3.1 Validation of modelled chlorophyll

The modelled annual mean surface chlorophyll in the CHL experiment with $\alpha = 1.15$ is firstly compared to the merged observed surface chlorophyll field from the GlobColor project (Maritorena et al. 2010), spanning the period from

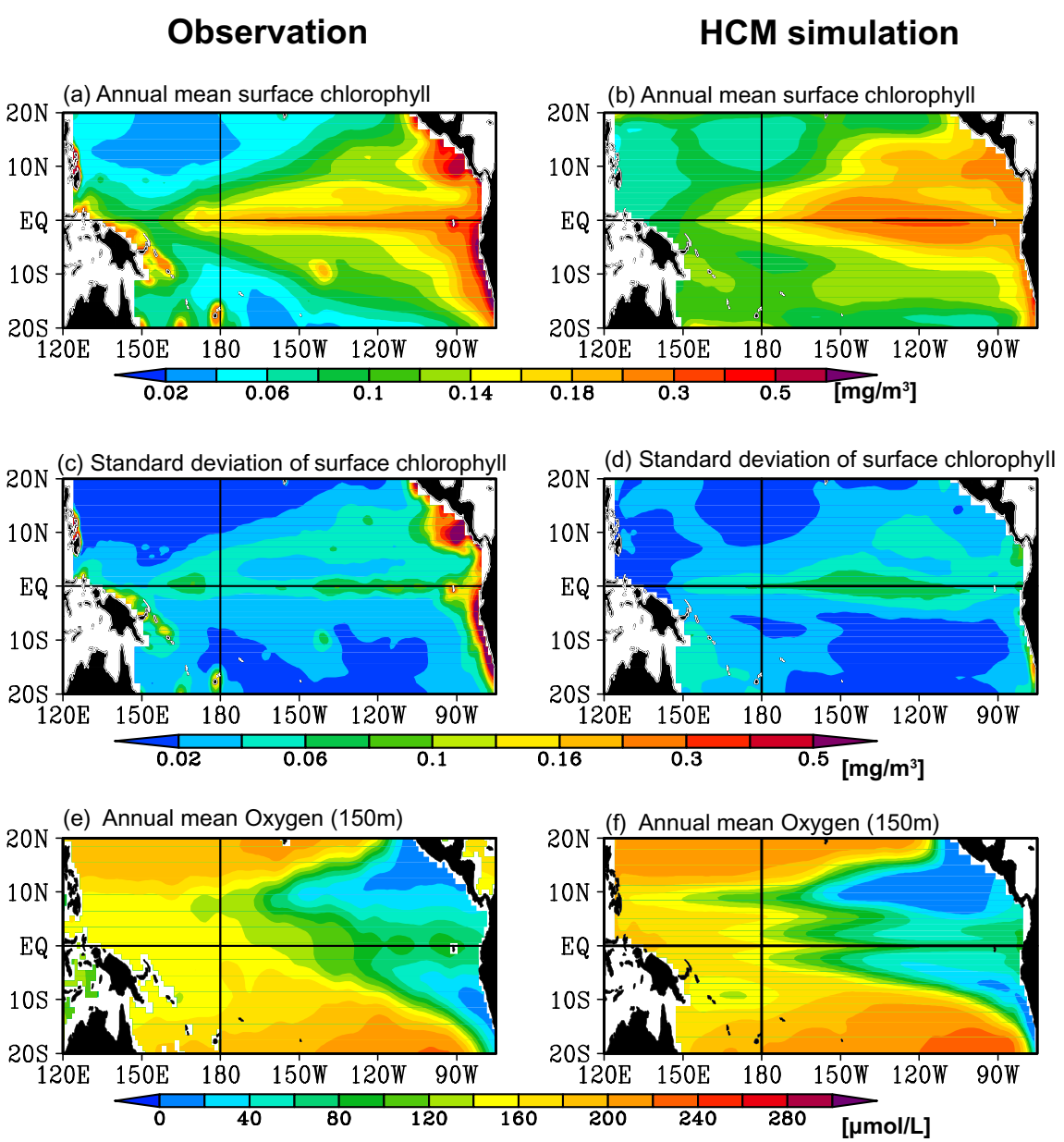

Fig. 1 Horizontal distribution of observed annual mean sea surface chlorophyll (**a**), standard deviations of interannual surface chlorophyll anomalies (**b**), and oxygen concentrations at 150 m (O_2, µmol L^{-1}) as a proxy for oxygen minimum zones (**c**); **d**–**f** are same as **a**–**c** but from the HCM simulation at $\alpha = 1.15$

1998 to 2016 (Fig. 1a and b). The coupled model can well simulate the major spatial distribution of surface chlorophyll, with elevated chlorophyll in the eastern equatorial Pacific, but low chlorophyll in the western equatorial and subtropical Pacific. The interannual variation of chlorophyll near the equator is large, which has been basically reproduced by the biogeochemical model in the central equatorial Pacific, but underestimated in the eastern equatorial region and north of the equator (Fig. 1c and d). It is noteworthy that the annual mean and interannual variations of modelled chlorophyll tend to be overestimated in the central-eastern equatorial region, which may be attributed to the stronger-than-observed equatorial upwelling and possible bias in the C:Chl ratio (Wang et al. 2009b). In addition, due to the inadequate representation of coastal processes such as land runoff and coarse resolution in the current ocean model, the modelled chlorophyll and its interannual variability tend to be underestimated in some coastal regions like the North and South America, where the chlorophyll concentration is high exceeding 1 mg m^{-3} (Fig. 1). Figure 1e and f show that the comparison of annual mean oxygen concentration at 150 m (as a proxy

for oxygen minimum zones (OMZs)) from WOA18 (Boyer et al. 2018) and model simulations. The model can basically reproduce the characteristic of OMZ in the eastern tropical Pacific. Overly, the focus of this study is on the sensitivity of chlorophyll-induced SST change in the open ocean. Thus, the good performances of the biogeochemical model in the open ocean waters are encouraging and adequate for this modelling study.

3.2 Influence of chlorophyll on the ocean mean state in the uncoupled (α = 0.0) and strongly coupled simulations (α = 1.15)

In this section, the effects of chlorophyll on the tropical Pacific mean-state SST under the condition without (α = 0.0) and with strong ocean–atmosphere coupling (α = 1.15) are examined. So, we can clearly investigate the role of ocean–atmosphere coupling in chlorophyll-induced SST change.

3.2.1 Uncoupled simulation (α = 0.0)

The presence of chlorophyll acts to absorb more solar radiation within the ML, with less radiation penetrating out of the bottom of the ML. We firstly adopt a diagnostic analysis developed by Zhang (2015) to examine the spatial distribution of annual mean chlorophyll-induced heating, including the absorbed solar radiation within the ML (Q_{abs}), and the related chlorophyll-induced direct heating rate on the ML (R_{sr}), and the penetrative solar radiation out of the bottom of the ML (Q_{pen}). These three terms can be calculated as follows:

$$Q_{abs}(H_m, H_p) = Q_{sr}\left[1 - \gamma \exp(-H_m/H_p)\right] \tag{2}$$

$$\begin{aligned} R_{sr}(H_m, H_p) &= Q_{sr}\left[1 - \gamma \exp(-H_m/H_p)\right]/(\rho_0 c_p H_m) \\ &= Q_{abs}/(\rho_0 c_p H_m) \end{aligned} \tag{3}$$

$$Q_{pen}(H_m, H_p) = Q_{sr}\left[\gamma \exp(-H_m/H_p)\right] \tag{4}$$

where Q_{sr} denotes the solar radiation arriving on the sea surface; $\gamma = 0.33$ denotes the fraction of solar radiation penetrating the sea surface by several centimeters, i.e., blue–green band (with wavelengths less than 550 nm). ρ_0 is the density of seawater, and c_p is the heat capacity. Thus, these three terms are determined by H_m (i.e., MLD) and penetration depth (H_p). In this study, the Q_{sr} is prescribed as its climatological field to emphasize the chlorophyll-induced solar radiation heating on the ocean.

Figure 2 shows the annual mean differences in these three heating terms between CHL and PURE with the uncoupled simulation (α = 0.0). As expected, the presence of chlorophyll tends to absorb more solar radiation within the ML (i.e., an increase in Q_{abs}), especially in the eastern equatorial Pacific, where the Q_{abs} difference induced by chlorophyll reaches + 5 W m^{-2} near the equator (Fig. 2a). Accordingly, the solar radiation penetrating out of the bottom of the ML (Q_{pen}) is decreased by − 5 W m^{-2} near the equator (Fig. 2c). The presence of chlorophyll tends to directly heat the ML and enhance the ocean stratification by modifying the relative distribution between Q_{abs} and Q_{pen}.

An increase in Q_{abs} leads to an increase in R_{sr} by more than 1 °C month^{-1} near the equator from 150° W to 100° W (Fig. 2b). It is anticipated that an increase in R_{sr} directly induces a warming effect on the ML and leads to an increase in SST by modifying the ML heat budget. However, as shown in Fig. 3a, under the condition without the ocean–atmosphere coupling (α = 0.0), the SST difference between CHL and PURE in the eastern equatorial Pacific is negative, indicating that the presence of chlorophyll acts to induce a cooling effect in the cold tongue. This result is similar to the previous study using ocean-only models (Nakamoto et al. 2001; Anderson et al. 2007; Park et al. 2014b; Lim et al. 2018). In addition, a slightly persistent warming emerges in the southern subtropical Pacific, whereas cold SST anomalies are maintained north of the equator in the range from 170° W to 140° W (Fig. 3a).

The increase in Q_{abs} tends to increase the surface buoyancy flux, leading to a shoaling of the ML (Fig. 4c). At α = 0.0, the ocean model is actually forced by prescribed climatological wind stress, and the shoaling of ML leads to a stronger Ekman divergence near the equator (Fig. 5c) as suggested by Sweeney et al. (2005) and Lim et al. (2018). The enhanced Ekman divergence further leads to a stronger upwelling and thus colder SST in the eastern equatorial Pacific (Fig. 3a). The SST cooling in the upper ocean is also associated with the shoaling of the thermocline (Fig. 5e, black and red lines), negative anomalies of sea level (Fig. 5c, color shaded). Therefore, direct heating effect induced by chlorophyll (Fig. 2) is ultimately overwhelmed by the indirectly induced dynamical cooling effect (Fig. 5c and e). Furthermore, an ML heat budget analysis is performed as follows.

$$\frac{\partial T}{\partial t} = -u\frac{\partial T}{\partial x} - v\frac{\partial T}{\partial y} - w\frac{\partial T}{\partial z} + Q_{mix} + Q_{net} \tag{5}$$

where $\frac{\partial T}{\partial t}$ is the tendency of the ML temperature; the first three terms on the right-hand side of Eq. (5) are zonal (uadv), meridional (vadv), and vertical advection (wadv), respectively; Q_{mix} represents the vertical entrainment and diffusion at the base of the ML, calculated based on a mixed layer model (Chen et al. 1994), which combines three major mechanisms of vertical turbulent mixing in the upper ocean

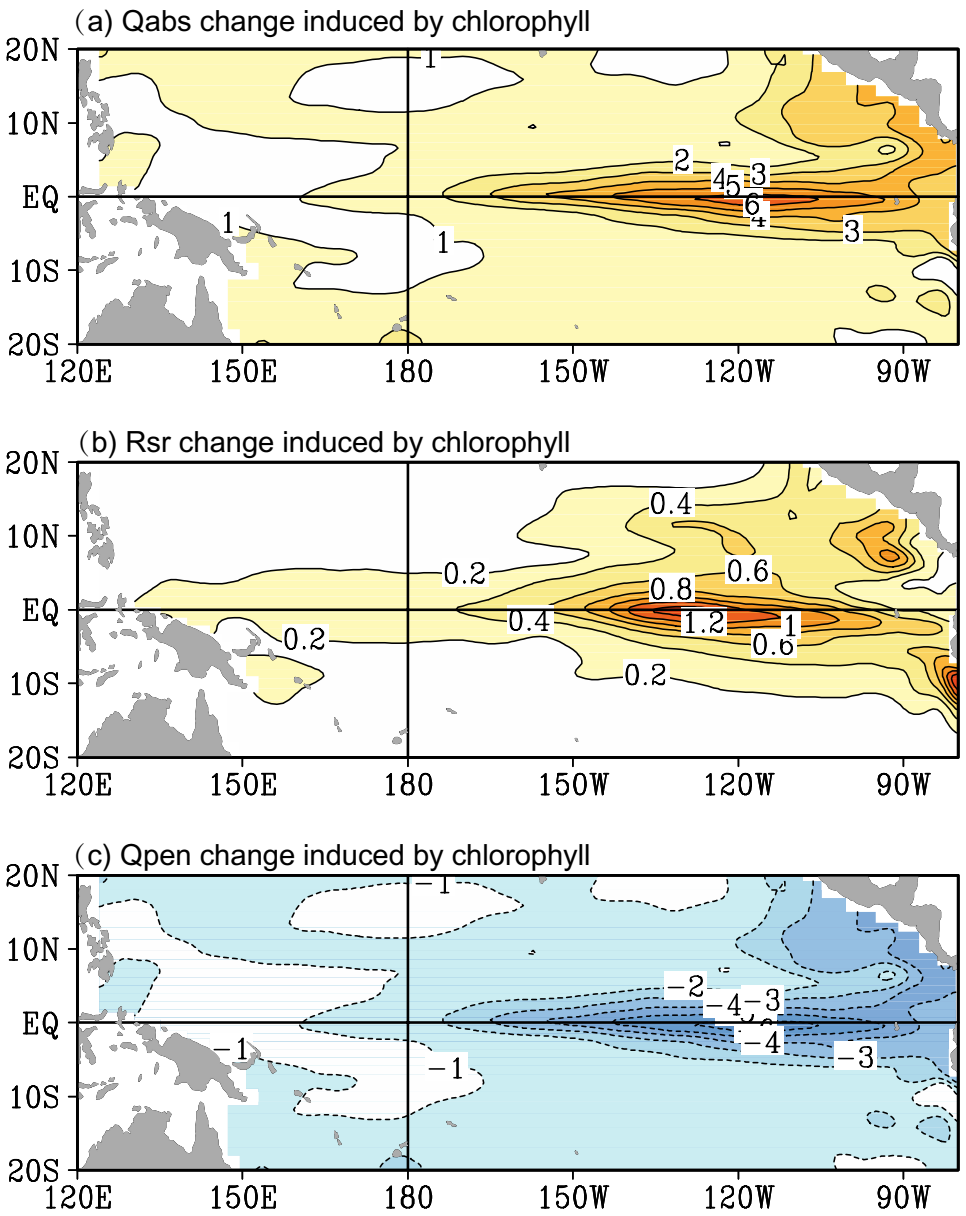

Fig. 2 Annual mean differences between CHL and PURE experiments for Q_{abs} (**a**), R_{sr} (**b**) and Q_{pen} (**c**). Q_{abs} indicates the absorbed solar radiation within the mixed layer; R_{sr} indicates the direct heating rate in the mixed layer induced by Q_{abs}; Q_{pen} indicates the penetrative solar radiation out of the bottom of the mixed layer. The contour intervals are 1 W m^{-2} in **a**, 0.2 ℃ $month^{-1}$ in **b** and 1 W m^{-2} in **c**, respectively

(wind stirring, shear instability, and convective overturning) (Kraus and Turner 1967; Price et al. 1986). To simplify the analysis, the sum of Q_{mix} and vertical advection is shown; Q_{net} is the net surface heat flux. In this ocean model, the surface heat flux is determined by an advective mixed layer model (Seager et al. 1995; Murtugudde et al. 1996), in which longwave radiation, latent and sensible heat flux are computed by wind, cloud cover and the ocean modeled SST. Note that in the ocean-only experiment ($\alpha = 0.0$), the wind stress is prescribed to be a climatological field in PURE and CHL, so that the change in surface heat flux is solely attributed to the SST change without considering the effect due to change from the surface wind.

In the western equatorial Pacific, the concentration of chlorophyll is relatively low (Fig. 1a). A decrease in penetration depth (H_p) induced by low chlorophyll (Fig. 4a) is compensated for by the ML shoaling (Fig. 4c), which leads to an small change in Q_{abs} as suggested in Eq. 2 (Fig. 2a), and nearly no change in net surface heat flux (< 1 W m^{-2}) (blue bars in Fig. 6a and c). Therefore, the SST in the western equatorial Pacific remains nearly no change at $\alpha = 0.0$ when the chlorophyll-induced effect is included (Fig. 3a).

In the eastern equatorial Pacific, the concentration of chlorophyll is relatively elevated due to the strong equatorial upwelling (Fig. 1a). High chlorophyll reduces the H_p by more than 10 m near the equator (Fig. 4a) and further leads to an increase in Q_{abs} by 4–6 W m^{-2} (Fig. 2a). The net surface heat flux increases by 8 W m^{-2} (blue bar in Fig. 6d), accounting for about 20% of the annual mean net

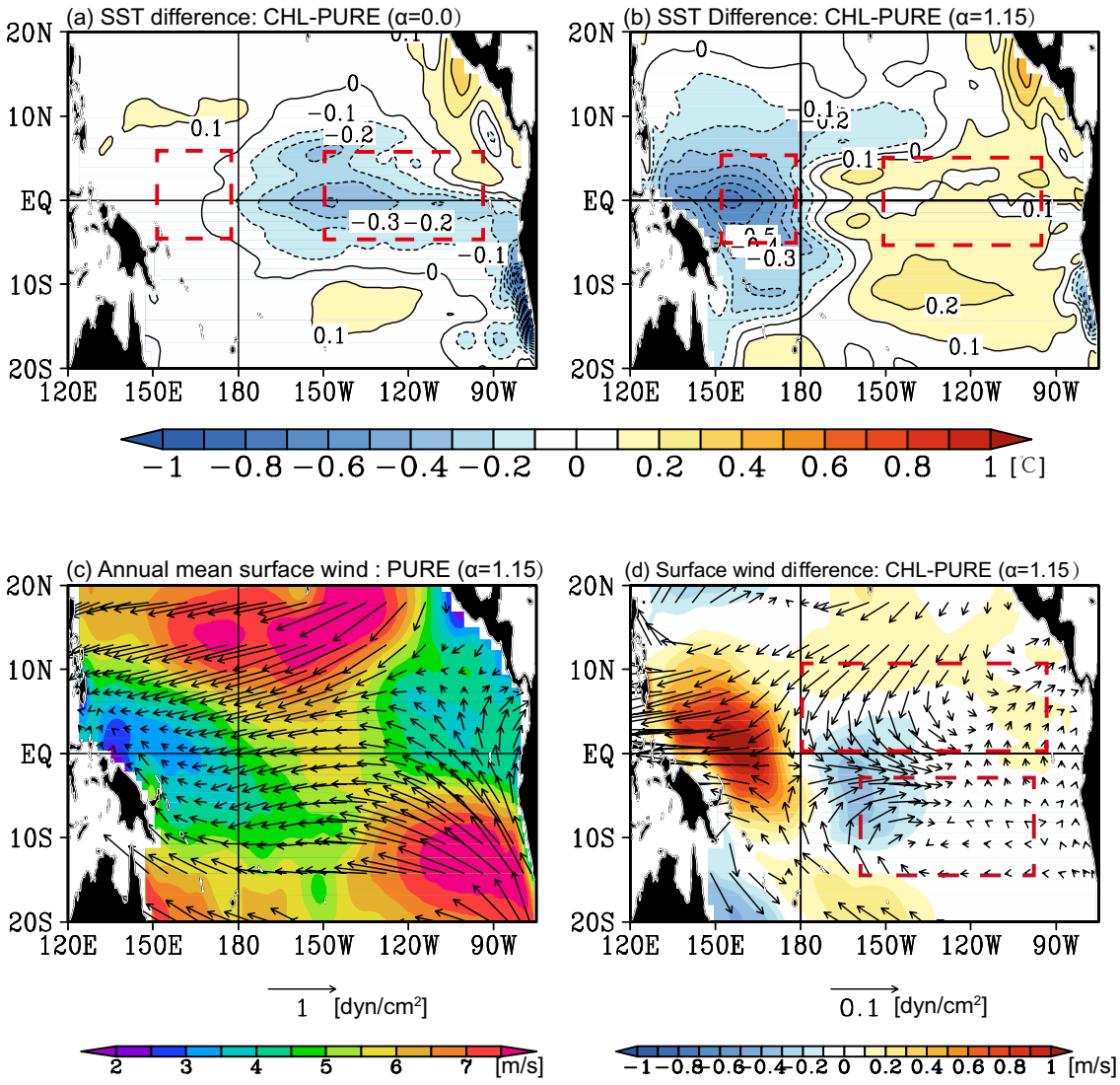

Fig. 3 Annual mean SST differences between CHL and PURE experiments with coupling intensity (α) for 0.0 (**a**), 1.15 (**b**); **c** is for the annual mean surface wind speed (shaded) and wind stress in PURE at α = 1.15; **d** is similar to **c** but for the difference between CHL and PURE at α = 1.15. Note that α = 0.0 indicates the ocean-only experiment forced by prescribed wind stress. The contour intervals are 0.1 °C in **a** and **b**. The red boxes represent the western Pacific (5° S–5° N, 155° E–175° E), the eastern Pacific (5° S–5° N, 150° W–90° W), the northern tropical Pacific (0°–10° N, 180°–90° W) and the southern subtropical Pacific (15° S–5° S, 160° W–100° W), respectively

surface heat flux. Correspondingly, the SST tendency can be increased by 0.4 °C month^{-1}. Simultaneously, cooling effects induced by meridional advection and vertical mixing are enhanced due to the intensification of Ekman divergence (Fig. 5c), which in turn overwhelms the increase in net surface heat flux (Fig. 6b), and consequently induces an SST cooling in the eastern equatorial Pacific.

It is noteworthy that the change in the latent heat flux tends to be positive and contributes significantly to the increase in net surface heat flux (Fig. 6d), which can be attributed to the negative feedback between the latent heat flux (LHF) and SST due to the exponential dependence of LHF on SST derived from the Clausius–Clapeyron relationship. However, due to the absence of the ocean–atmosphere coupling, the strengthened ocean dynamical cooling effect dominates the ultimate SST change in the eastern equatorial Pacific at α = 0.0.

3.2.2 The strongly coupled condition (α = 1.15)

As shown in Fig. 3a, the presence of chlorophyll acts to induce an SST cooling in the eastern equatorial Pacific when taking α = 0.0 (i.e. no ocean–atmosphere coupling). Thus, this cooling effect is expected to be amplified when

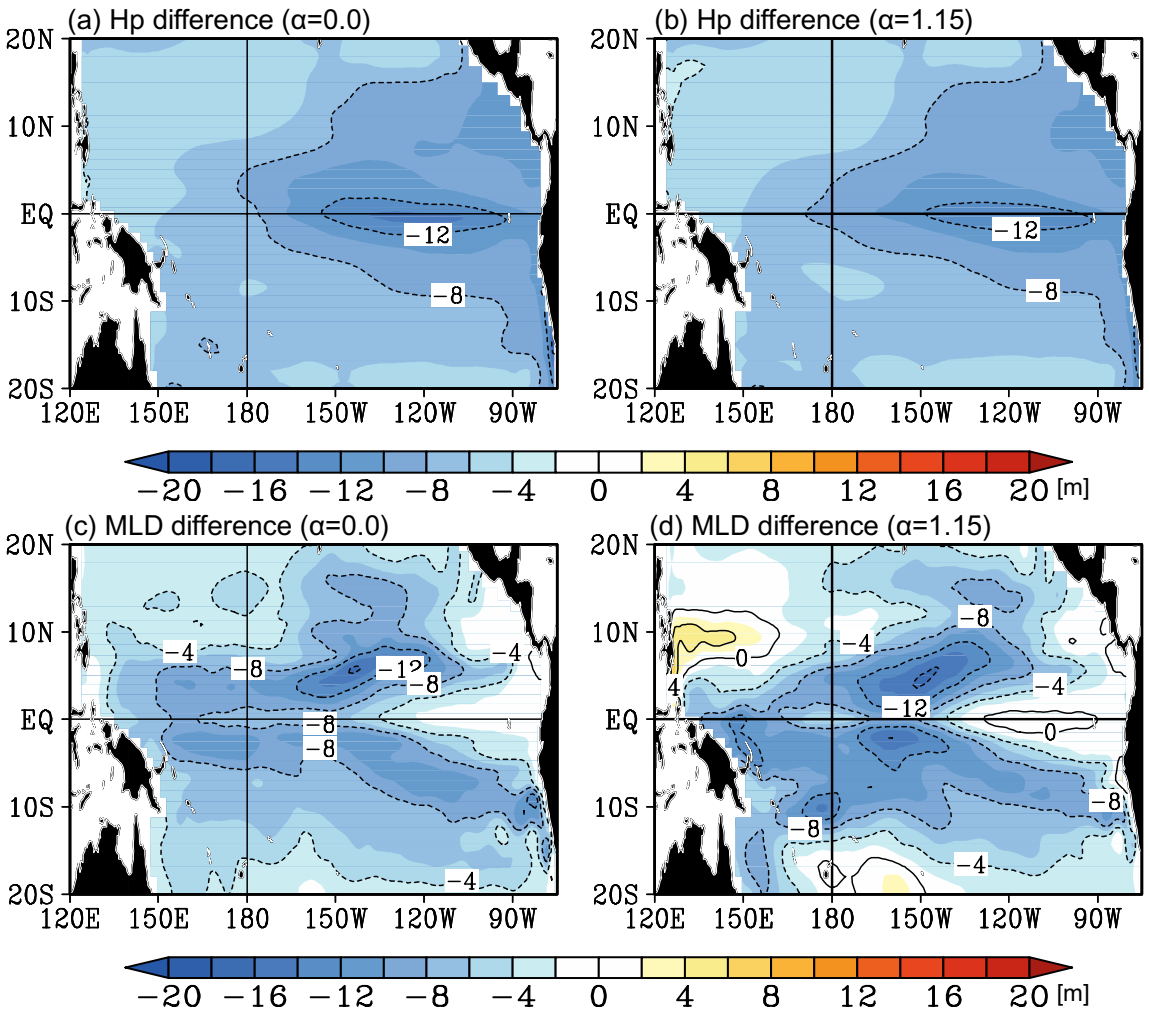

Fig. 4 Annual mean differences in H_p for **a**, **b**, MLD for **c**, **d** between CHL and PURE experiments at α = 0.0 (left panels) and α = 1.15 (right panels). The contour intervals are 4 m in **a**–**d**

the large-scale ocean–atmosphere coupling is represented through the positive Bjerknes feedback, which has been found in a simulation using the GFDL-CM 2.1(e.g., Park et al. 2014a). However, in our HCM simulation, by taking α = 1.15, the presence of chlorophyll actually induces an SST warming in the eastern equatorial Pacific when the ocean–atmosphere coupling is explicitly taken into account (Fig. 3b), characterized by an El Niño-like pattern. Furthermore, SST warming induces anomalous westerly winds in the central equatorial Pacific, with wind speed decreasing by 0.6 m s^{-1} south of the equator (Fig. 3d). Correspondingly, an anomalous SST cooling emerges in the western equatorial Pacific and north of the equator in association with anomalously easterly winds and an increase in wind speed (Fig. 3b and d), which may be attributed to the cyclonic wind curl associated with Rossby-wave response to SST warming in the central-eastern Pacific (170° W–140° W). Also, the western equatorial Pacific (155° W–170° W) cooling also maintains and can generate anomalous easterly winds according to Gill-type pattern (Gill 1980). In the southern subtropical Pacific, a persistent warming also emerges in this coupled case (α = 1.15), while cold SST anomalies are maintained north of the equator in the range from 170° W to 140° W (Fig. 3b). The north–south difference in SST further induces cross-equatorial northerly winds in the central Pacific and winds to shift eastward south of the equator due to the Coriolis effect (Fig. 3d). Furthermore, the slow-down of the trade winds in the southern subtropical Pacific leads to a reduction in the evaporative cooling, thereby strengthening the warming in the off-equatorial eastern Pacific. Therefore, the eastern tropical Pacific SST warming can be strengthened by the wind-evaporation-SST mechanism as suggested by Xie and Philander (1994).

In terms of the persistent warming in the southern tropical Pacific, it is well known that the mixed layer (ML) is

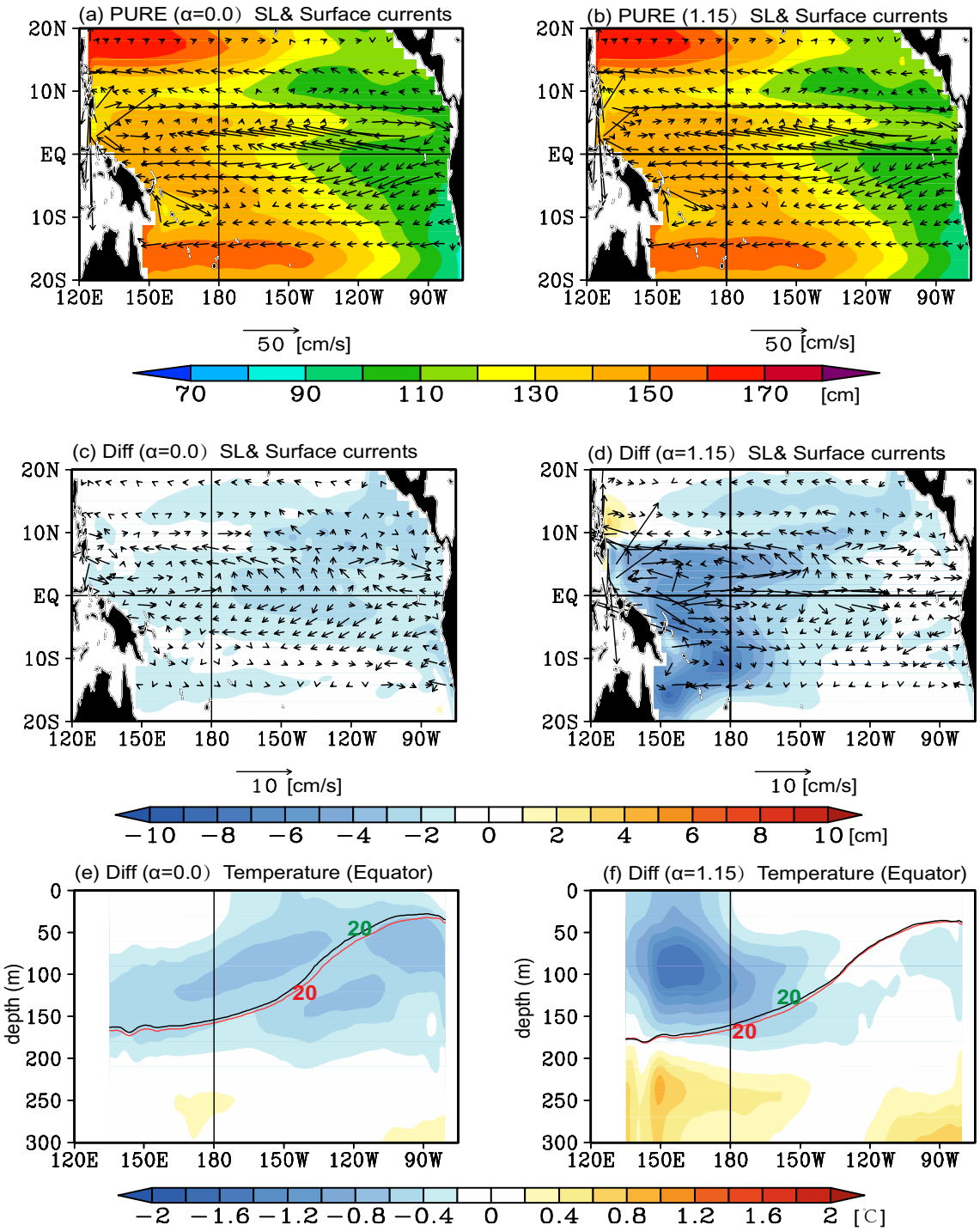

Fig. 5 Annual mean surface current (vectors) and sea levels (SL, shaded) in CHL at α = 0.0 (**a**) and α = 1.15 (**b**); the corresponding differences between CHL and PURE experiments at α = 0.0 (**c**) and α = 1.15 (**d**); **e** and **f** are similar to **c** and **d** but for the temperature difference along the equator. The red and black line in **e**, **f** denotes the 20 ℃ isotherm in PURE and CHL experiments, respectively

relatively deep in the southern tropical Pacific associated with the formation of high salinity water mass. The deep mixed layer inhibits the solar radiation penetrating out of its bottom, thus the chlorophyll-induced change in the penetrative solar radiation (Q_{pen}) is tiny and most of the solar radiation is absorbed within the entire mixed layer (Q_{abs}). Therefore, the chlorophyll acts to induce a warming effect in the southern subtropical Pacific. For the SST cooling in the northern tropical Pacific as shown in Fig. 3, we speculate some reasons as follows. The presence of chlorophyll acts to

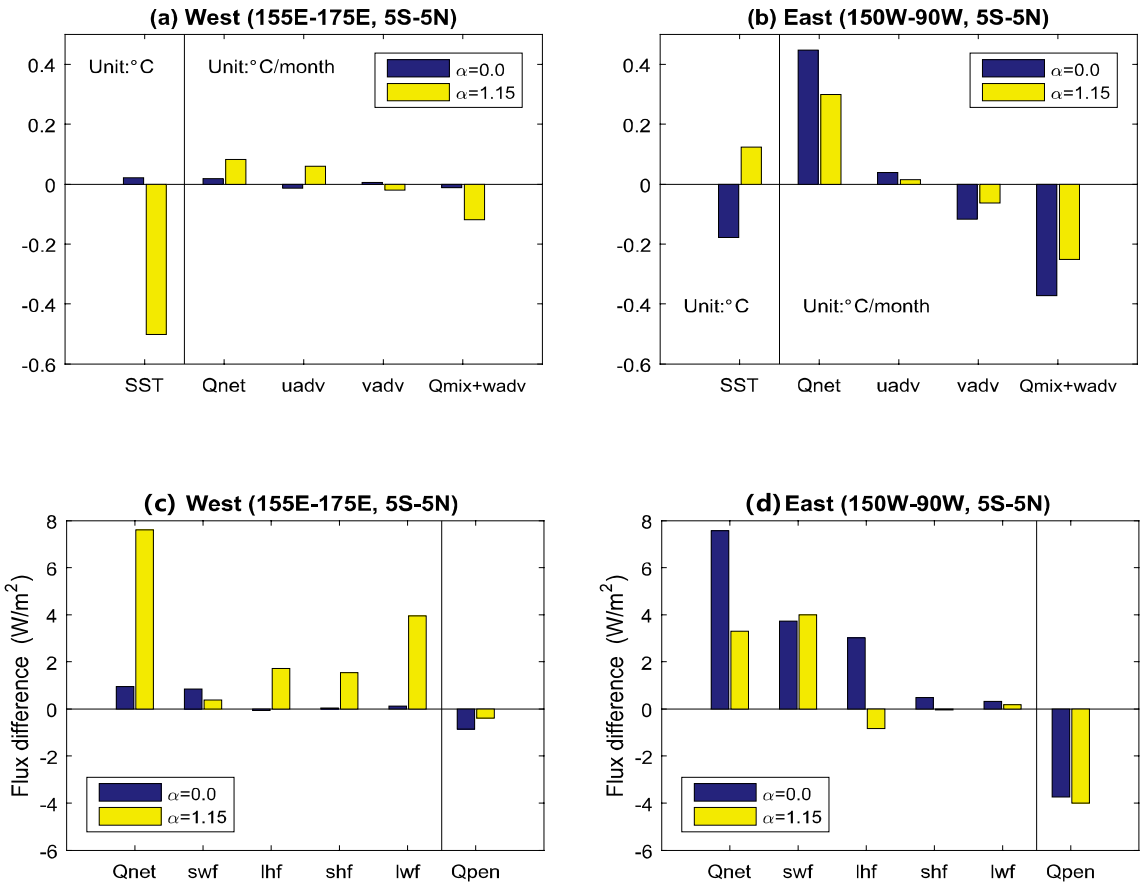

Fig. 6 The differences in the mixed layer heat budget between CHL and PURE experiments with α = 0.0 (uncoupled, blue bars) and α = 1.15 (coupled, yellow bars), averaged over the western equatorial Pacific (155° E–175° E, 5° S–5° N) in **a**, the eastern equatorial Pacific (150° W–90° W, 5° S–5° N) in **b**; **c** and **d** are for the decomposition analysis of surface heat fluxes (net surface heat flux (Q_{net}), absorbed shortwave radiation flux within the mixed layer (swf), longwave radiation flux (lwf), latent heat flux (lhf), sensible heat flux (shf) and penetrative solar radiation out of bottom of the mixed layer (Q_{pen})) over the western region and eastern region, respectively. Note that the shortwave radiation here denotes the absorbed part within the mixed layer (i.e., Q_{abs})

enhance the shortwave-induced heating within the ML and leads to a shoaling of the ML. As described in the Introduction, the shoaling of the ML indirectly strengthen the subtropical-tropical cell and further leads to an enhanced south equatorial current (SEC), which can result in the cooling north of the equator. Meanwhile, due to the strengthening of the SEC, the current shear also can be enhanced, which in turn leads to an enhanced tropical instability wave (TIWs) (Löptien et al. 2009). Enhanced TIWs tend to transport more cold waters northward and induces a cooling effect in the northern tropical Pacific (Jochum et al. 2007; Graham 2014). Note that the related mechanism in terms of persistent cooling (warming) in the northern (southern) tropical Pacific still needs to be investigated in the future.

Figure 4b shows that the spatial difference in H_p between CHL and PURE in the coupled condition (α = 1.15) is identical to that at α = 0.0, indicating that H_p exhibits nearly no change between uncoupled and coupled cases (Fig. 4a, b). In other words, the atmospheric feedback cannot significantly affect the biological response (i.e., the chlorophyll change), which further makes little contribution to the change in H_p. The difference in MLD is also similar to that at α = 0.0 in the equatorial Pacific, and leads to a similar change in Q_{abs} (Eq. 2; figure not shown). The change in MLD is tiny in the eastern equatorial Pacific in the coupled and uncoupled condition attributed to the adjustment of ocean circulation (Fig. 5). Thus, the presence of chlorophyll actually leads to an increase in Q_{abs} and a decrease in Q_{pen}. Certainly, the coupling between dynamical process and biological processes within the mixed layer needs to be investigated in detail. For example, using a 1-D coupled model between physics and biology may clearly identify the specific processes, which is still a fundamental question for bio-physical coupling.

In the western tropical Pacific, ocean currents exhibit remarkable change, with an anomalously eastward surface current near the equator in association with a negative sea level anomaly (Fig. 5d). The anomalously eastward surface current leads to an enhanced zonal temperature advection,

which contributes to the warming of SST in the central Pacific. In the western tropical Pacific, anomalous easterlies winds tend to induce an enhanced Ekman divergence and upwelling. Thus, the subsurface cool water is easily upwelled into the surface layer (Fig. 5f), which consequently leads to a decrease in SST. As shown in Fig. 6a, intensified vertical mixing dominates the ML temperature budget, which leads to the SST cooling, while the net surface heat flux and zonal temperature advection tend to warm the mixed layer in the western equatorial Pacific. It is noteworthy that the change in the net surface heat flux is positive, reaching 8 W m^{-2} (Fig. 6c). Due to the small change in the Q_{abs}, the change in the net surface heat flux is mainly attributed to the increase in the latent, sensible heat fluxes and longwave radiation, while the latent heat flux (LHF) feedback plays a key role in determining the change of the net surface heat flux in the western Pacific (Fig. 6c). In total, the cooling effect induced by the enhanced vertical mixing overwhelms the warming effect due to the increase in the net surface heat flux, subsequently leading to an SST cooling in the western equatorial Pacific.

In the central-eastern equatorial Pacific, anomalously westerly winds tend to reduce the zonal SST gradients, and in turn warm SST anomalies enhance the westerlies (Fig. 3b and d), which further exerts a positive feedback, i.e. Bjerknes feedback (Bjerknes 1969). In addition, the subsurface temperature exhibits no change in association with nearly zero change of the thermocline depth east of 130°W, but some change in thermocline depth and subsurface warming in the central Pacific, when the effect of chlorophyll is included in CHL (Fig. 5f). The vertical mixing and meridional advection are also decreased due to the weakened wind stress (Fig. 3d), indicating that ocean dynamical cooling effect induced by chlorophyll tends to be weakened. As shown in Fig. 6d, the difference in net surface heat flux is decreased to about 3 W m^{-2} at $\alpha = 1.15$, which is less than a half of that when taking $\alpha = 0.0$. Owing to unchanged value in Q_{abs}, the decrease in net surface heat flux is primarily attributed to the decrease in latent heat flux. As suggested in the previous section, latent heat flux is computed by an atmosphere mixed layer model, being interactively dependent on the change in the SST and wind speed. An increase in SST tends to decrease the latent heat flux due to negative relationship as suggested in Haney (1971). In addition, the decrease in wind speed tends to amplify this negative latent flux anomalies and consequently leads to a decrease in the latent heat flux by -1 W m^{-2}. However, although the net surface heat flux is reduced, vertical mixing and upwelling weaken more, resulting in the net SST warming in the eastern equatorial Pacific.

In short summary, the SST change due to the existence of chlorophyll is highly dependent on the relative contribution from the direct warming effect due to net surface heat flux and indirect cooling effect due to ocean dynamics. In the uncoupled case ($\alpha = 0.0$), the ocean dynamical cooling plays a dominant role in determining the change of SST in the eastern equatorial Pacific. In the coupled case ($\alpha = 1.15$), the surface warming induced by direct heating associated with the presence of chlorophyll acts to suppress the ocean dynamical indirect cooling, with their net effects leading to the SST warming in the eastern equatorial Pacific. Additionally, we found that in the strong coupling condition ($\alpha = 1.15$) without chlorophyll effect, an El Niño-like pattern emerges in the tropical Pacific, with an SST cooling in the western equatorial Pacific and an SST warming in the eastern equatorial Pacific (figure not shown), as compared with that in uncoupled condition ($\alpha = 0.0$). This pattern can be attributed to the residual effect due to ENSO asymmetry with larger positive SST anomalies during El Niño phase. Furthermore, the presence of chlorophyll tends to amplify this residual warming effect, which in turn indirectly demonstrates the robustness of chlorophyll-induced heating under strongly coupling condition. At this stage, the reason why there is a remarkable change in SST response from cooling to warming has been discussed. However, whether is there a threshold at which SST in the tropical Pacific can have a sign change due to the presence of chlorophyll and ocean–atmosphere interaction? This question will be investigated in the next subsection utilizing more HCM-based experiments.

3.3 Chlorophyll-induced effects on the SST that are dependent on the ocean–atmosphere coupling intensity (α)

In this section, the ocean–atmosphere coupling intensity is further tuned to illustrate the possible existence for thresholds at which the effects of chlorophyll on the mean state SST can change the sign.

Figure 7 shows the SST differences between CHL and PURE at different coupling intensity with α ranging from 0.5 to 1.10. During the weakly represented coupling case ($\alpha \leq 1.0$, Fig. 7a–c), the spatial patterns of SST differences are basically similar to those in the uncoupled case ($\alpha = 0.0$, Fig. 3a), except for the smaller SST differences in the far eastern equatorial Pacific (east of 120ºW), where the SST cooling disappears (Fig. 7a–c). With the gradual increase in α, the negative SST differences alternatingly diminish westward along the equator (Fig. 7d–f). Meanwhile, the SST cooling gradually appears in the western equatorial Pacific. It is noted that the persistent warming (cooling) centers are still located in the south (north) of the equator, which is unaffected by the change in the increased coupling intensity. This asymmetric SST response further induces the cross-equatorial northerly winds in the central equatorial Pacific (Fig. 8). The SST warming south of the equator is

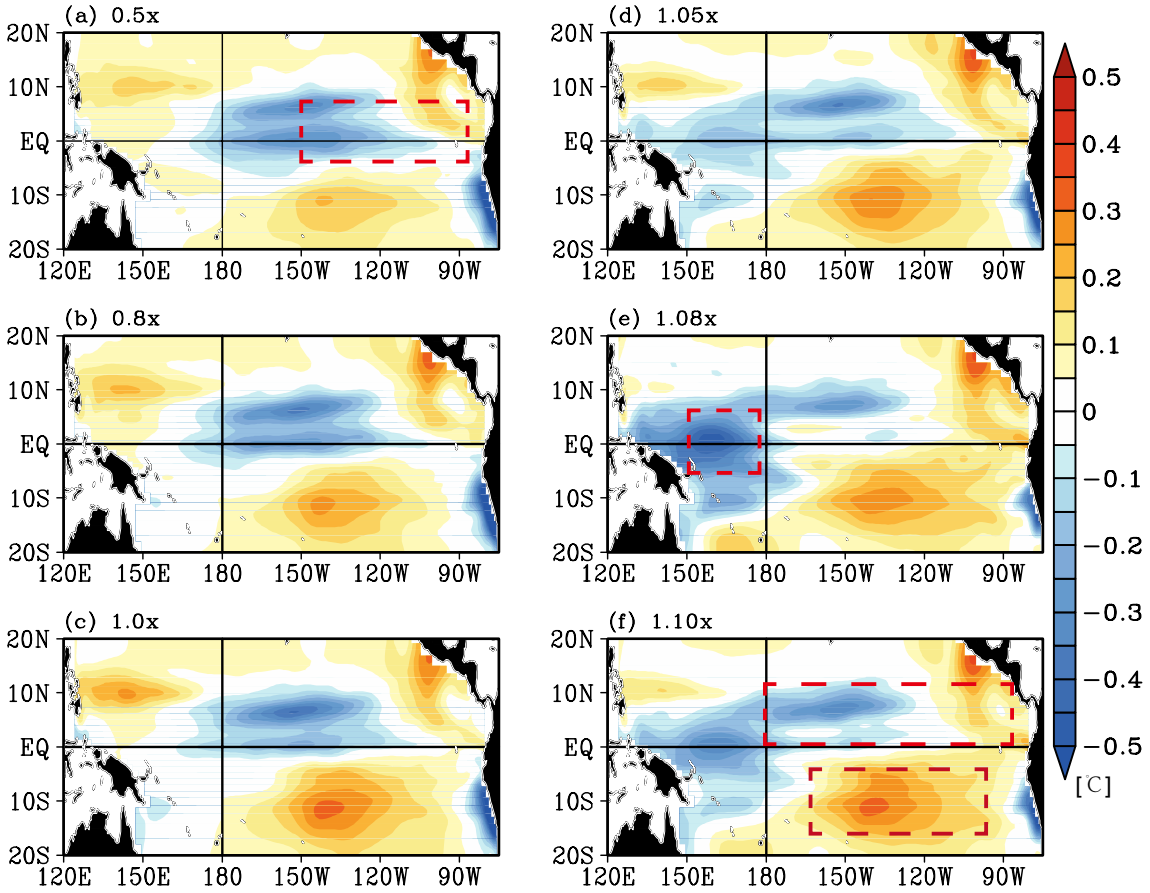

Fig. 7 Annual mean SST differences between CHL and PURE experiments with different coupling intensity; α = 0.5 (**a**), α = 0.8 (**b**), α = 1.0 (**c**), α = 1.05 (**d**), α = 1.08 (**e**) and α = 1.10 (**f**). The red boxes represent the western Pacific (5° S–5° N, 155° E–175° E), the eastern Pacific (5° S–5° N, 150° W–90° W), the northern tropical Pacific (0°–10° N, 180°–90° W) and the southern subtropical Pacific (15° S–5° S, 160° W–100° W), respectively

maintained by the decreased wind speed, and even is further amplified through the strengthened WES feedback (Xie and Philander 1994) (Fig. 8). Meanwhile, the SST cooling in the central equatorial Pacific acts to induce anomalous easterly winds, which results in an enhanced Ekman divergence and intensify the SST cooling effect west of the dateline. With the increase in the coupling intensity, the anomalous easterly wind gradually strengthens and further enhances the intensity of upwelling in the western equatorial Pacific. Subsequently, the difference in the zonal gradient of SST can be amplified through the Bjerknes feedback; the cross-equatorial northerly is also intensified due to the WES feedback.

As shown in Fig. 7, a transition state takes place from cooling to warming in the eastern equatorial Pacific when taking α = 1.0–1.1. Thus, we perform detailed sensitivity experiments by taking more values of α between 1.0 and 1.1, with the intervals increased by 0.01. As shown in Fig. 9b, when the value of α is set to larger than 1.01, the SST difference begins to reverse from negative perturbations to positive perturbations in the eastern equatorial Pacific (represented by averaged SST over the Niño3 region). It is noted that the threshold of 1.01 may slightly depend on the selected area but the main characteristic of SST changes due to varying coupled intensity is still clear as shown in Figs. 3 and 7. Because the significant change in SST over the Niño3 region, we select this region as the eastern box. With the increase in the coupling intensity, the positive SST perturbations gradually intensify, reaching 0.1 °C when taking α = 1.15. In the western equatorial Pacific, the SST cooling emerges (α = 0.8) and is further amplified when taking α > 1.03 (Fig. 9a). Therefore, within the HCM system, thresholds for SST changes can be identified when the coupling intensity attains to certain values (α = 1.01), at which the effect of chlorophyll on SST in the eastern equatorial Pacific can be reversed from cooling to warming.

Furthermore, detailed heat budget analyses for cases ranging from α = 0.0 to 1.15 are conducted in the eastern box (150° W–9° W, 5° S–5° N) and are illustrated in Fig. 10. With the increase in α, the change in net surface heat flux (blue line in Fig. 10a) between CHL and PURE

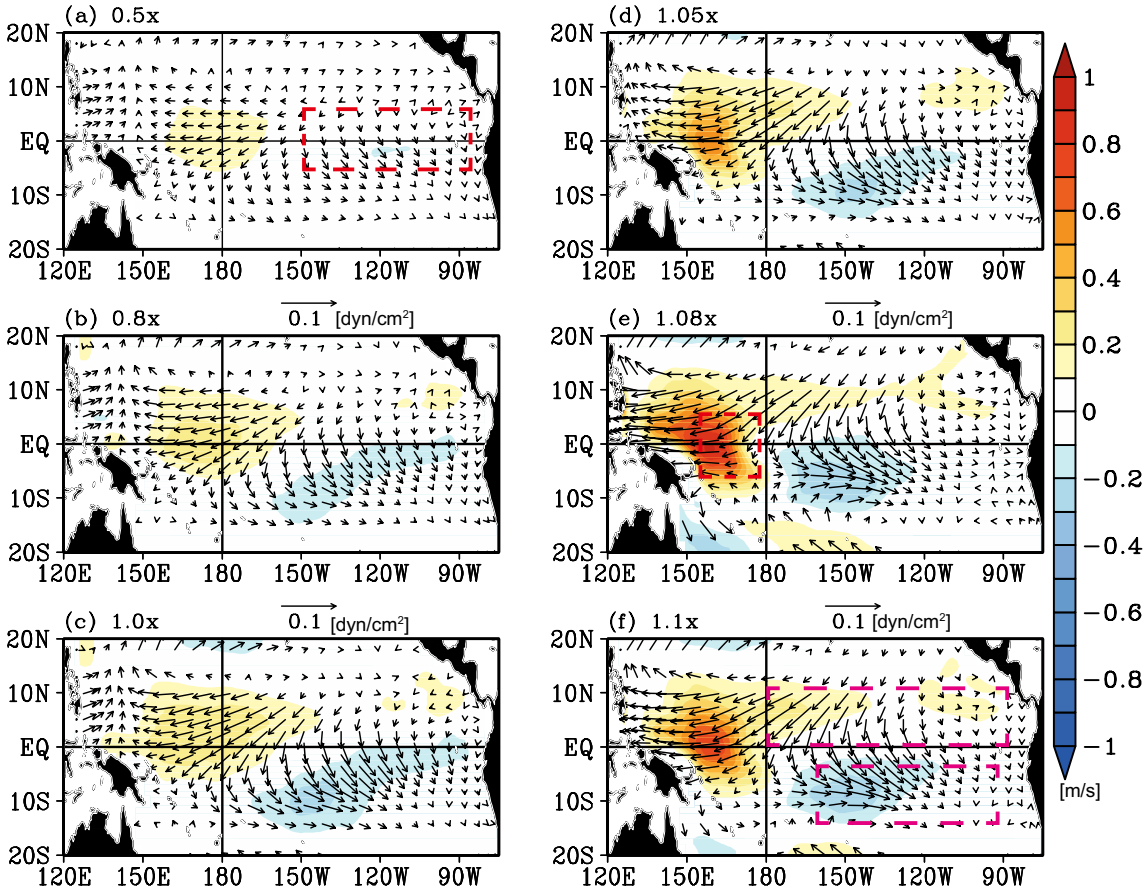

Fig. 8 The differences in annual mean wind speed (shaded) and wind stress (vectors) between CHL and PURE experiments with different coupling intensity; α = 0.5 (**a**), α = 0.8 (**b**), α = 1.0 (**c**), α = 1.05 (**d**), α = 1.08 (**e**) and α = 1.10 (**f**)

tends to decrease from 0.45 ℃/month at α = 0.0 to 0.35 ℃/month at α = 1.15, suggesting that the chlorophyll-induced direct heating gradually weakens in association with enhanced coupling intensity (Fig. 10a). Meanwhile, the vertical mixing and entrainment (red line in Fig. 10a) due to the adjustment of the ocean circulation and subsurface entrainment processes also decrease from − 0.4 ℃/month at α = 0.5 to − 0.25 ℃/month at α = 1.15, indicating the chlorophyll-induced indirect cooling is weakened more. Additionally, the meridional temperature advection also weakens from − 0.12 ℃/month at α = 0.0 to − 0.06 ℃/month at α = 1.15 (pink line in Fig. 10b). Although the contribution from meridional temperature advection to the indirect cooling is small, its role in balancing the heat budget within the mixed layer in the eastern equatorial Pacific cannot be overlooked. With the increase in the coupling intensity, the decrease in meridional temperature advection further weakens the indirect cooling effect induced by chlorophyll. As for the zonal advection (black line in Fig. 10b), its contribution is diverse and relatively small (0.01 to 0.05 ℃/month) in the heat budget change, which may be attributed to the weakening of mean current and temporal variability.

With the increase in coupling intensity, the relatively smaller chlorophyll-induced change in direct heating and dynamical cooling may be involved in the interaction between biology and climate; i.e., with the increase in α (coupling intensity), the initial warming induced by chlorophyll tends to induce anomalous westerly winds in the eastern equatorial Pacific. Anomalous westerly winds act to suppress the Ekman divergence in the eastern equatorial Pacific and further weakens the dynamical cooling effect. Meanwhile, the latent heat flux is reduced due to a decrease in wind speed. Therefore, as shown in Fig. 10, with the increase in α (coupled intensity), the chlorophyll-induced direct warming (change in net surface heat flux) and indirect cooling (advection and vertical mixing) both weaken, but the reduced amplitude of direct warming due to the changes in net surface heat flux is relatively small compared to the change in indirect dynamical cooling, and consequently leading to a dominant warming effect in the eastern tropical Pacific.

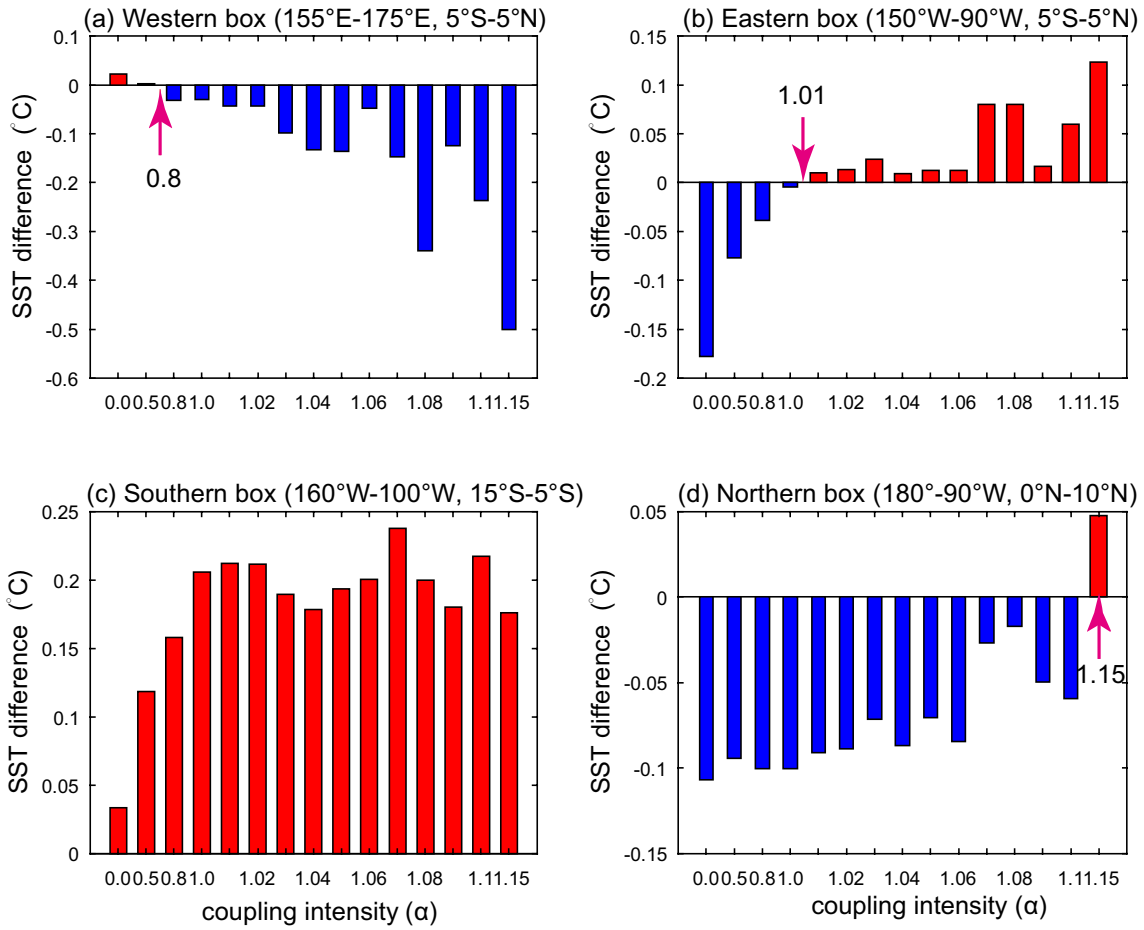

Fig. 9 The SST differences in the selected regions with different coupling intensity ranging from α = 0.0 to 1.15: **a** the western equatorial Pacific (155° E–175° E, 5° S–5° N); **b** the eastern equatorial Pacific (150° W–90° W, 5° S–5° N); **c** the South Pacific (160° W–100° W, 15° S–5° S); **d** the North Pacific (180° W–9° W, 0°–10° N). The intervals of α are 0.01 from 1.0 to 1.1 to detect the possible thresholds of SST change (α = 0.8 in **a**, α = 1.01 in **b** and α = 1.15 in **d**, respectively)

It is noted that the differences in SST due to the presence of chlorophyll are also dependent on the seasonality of ocean–atmosphere coupling. In the eastern tropical Pacific, the coupling intensity is large during boreal spring–summer and small during boreal fall-winter due to the interactions among SST, winds, and the mixed layer dynamics (Xie 1994; Chang 1996). However, the seasonal variations of H_p (or chlorophyll) are very weak as observed (Zhang et al. 2019b), with small positive chlorophyll anomalies (0.02 mg m^{-3}) emerging during boreal spring-summer time (spring phytoplankton bloom), attributed to enhanced vertical mixing and relative high SST. Previous studies suggest that the penetration of solar radiation may contribute to the seasonal cycle of SST in the eastern equatorial Pacific (Schneider and Zhu 1998). Interestingly, the presence of chlorophyll tends to induce persistent cooling during an entire year in the case without ocean–atmosphere coupling (α = 0.0) (Fig. 11a). Also, in the far eastern equatorial Pacific, during the boreal winter (December to February), the chlorophyll-induced direct heating may be offset by the indirect cooling as suggested previously (Fig. 11a). At α = 1.06 (Fig. 11b), with a moderate coupling intensity, the results show that the cooling is still maintained from April to August in the central equatorial Pacific, but the warming starts to emerge in the far eastern equatorial Pacific from January to March. At α = 1.15 (Fig. 11c), the chlorophyll-induced direct heating is further amplified in the boreal winter through the ocean–atmosphere coupling; from April to August, the direct heating induced by chlorophyll can still be compensated for by the indirect cooling which exhibits no change in the central-eastern equatorial Pacific (Fig. 11c). Thus, the change in the seasonal cycle of SST due to varying coupling intensity may further rectify the mean state of SST in the tropical Pacific. Additionally, the role of interannual variability of chlorophyll is not investigated in this study (Zhang et al. 2018b), and the impacts of multi-scale chlorophyll variability on the tropical Pacific mean state are shown elsewhere.

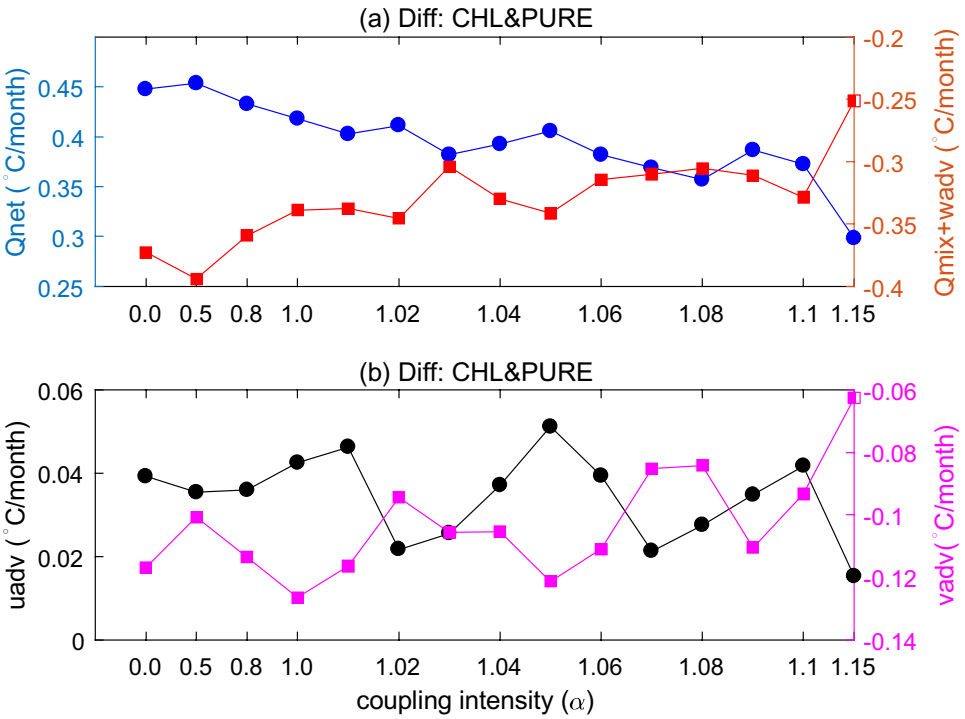

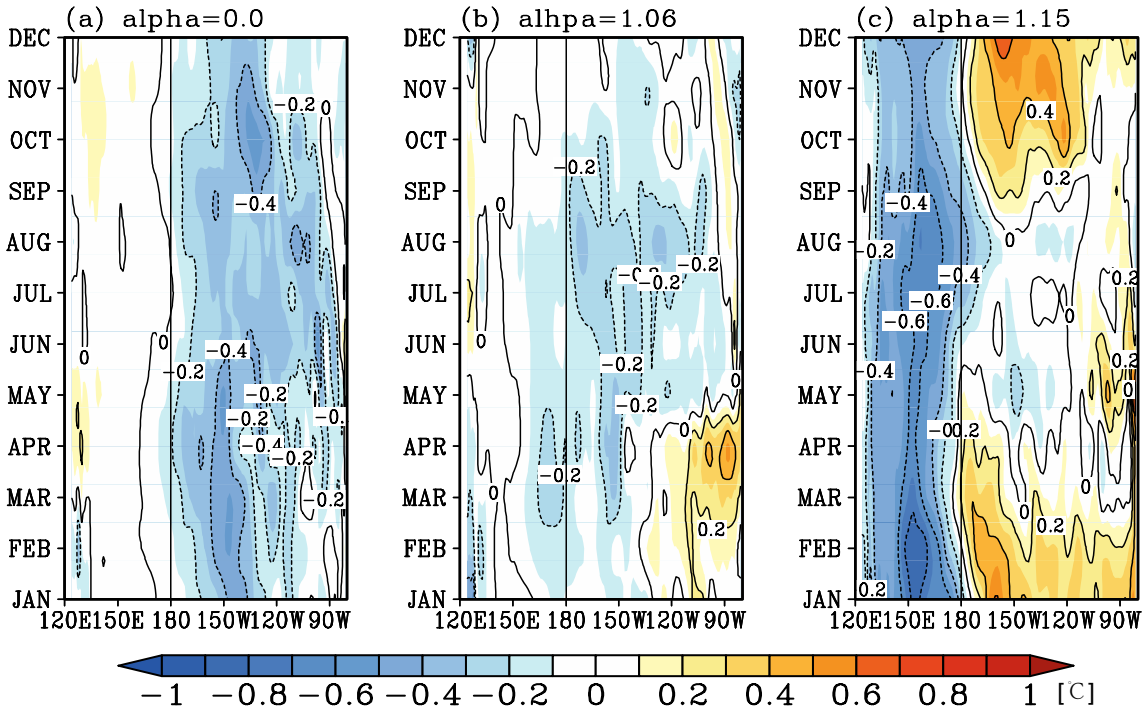

Fig. 10 The differences in the mixed layer heat budget between CHL and PURE experiments averaged over the east region (150° W–90° W, 5° S–5° N) with different coupling intensity ranging from α = 0.0 to 1.15, **a** net surface heat flux (blue curve) and vertical mixing (red curve), **b** zonal (black curve) and meridional temperature advection (pink curve)

Fig. 11 Time–longitude seasonal cycle for SST differences between CHL and PURE experiments with coupling intensity α = 0.0 (**a**), α = 1.06 (**b**) and α = 1.15 (**c**). The contour intervals are 0.2 °C

4 Summary and discussion

4.1 Summary

In this study, we examined the effects of chlorophyll on the mean state in the tropical Pacific using a hybrid coupled model (HCM) of the atmosphere, ocean physics and biogeochemistry, in which the ocean–atmosphere coupling intensity is allowed to change as represented by α. In the case without ocean–atmosphere coupling (i.e. α = 0.0; the ocean-only experiment), the presence of chlorophyll tends to induce a cooling effect on SST in the eastern equatorial Pacific, which is consistent with previous studies (Nakamoto et al. 2001; Löptien et al. 2009; Park et al. 2014a). When the ocean–atmosphere coupling is taken into account (α > 0.0), the chlorophyll-induced SST cooling effect in the eastern Pacific is gradually diminished as the coupling intensity increases. In the case with α > 1.01, an SST warming emerges instead in the eastern Pacific, accompanied by a cooling effect in the western equatorial Pacific; this El Niño-like SST response in the presence of chlorophyll effect is further amplified through the Bjerknes feedback in association with increasing α. Therefore, the chlorophyll effects on the tropical Pacific mean states are sensitively dependent on the coupling intensity between the ocean and atmosphere. Thresholds for coupling intensity can be detected nearly at α = 1.01, at which the corresponding chlorophyll effect on

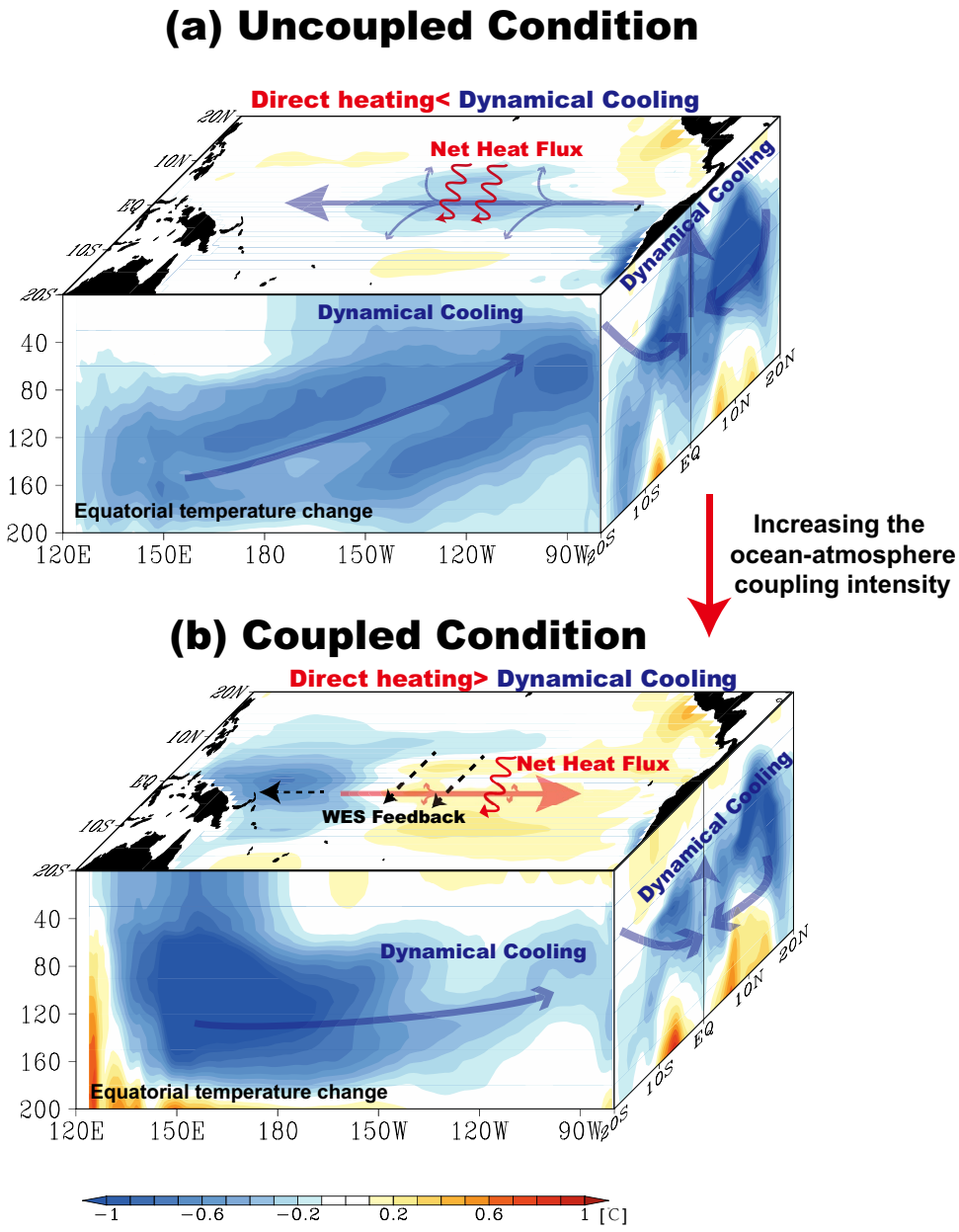

Fig. 12 A schematic of the SST change in response to the presence of chlorophyll under the condition without and with the ocean–atmosphere coupling. **a** In the case with no ocean–atmosphere coupling (i.e. α = 0.0), the presence of chlorophyll tends to induce a cooling effect in the eastern equatorial Pacific; indirectly dynamical cooling processes (the adjustment of ocean circulation (blue arrow), enhanced vertical mixing and upwelling) tend to dominate the SST cooling. **b** In the strong coupling cases, the chlorophyll-induced direct heating within the mixed layer plays a key role in maintaining the SST warming. In the off-equatorial central Pacific, a persisted cooling condition north of the equator and a warming condition south of the equator act to induce cross-equatorial northerly winds (black dash arrow) due to the WES mechanism. This cross-equatorial northerly winds shift eastward and further weakens the trade winds; the decrease in wind speed suppresses the LHF feedback and further leads to an increase in SST south of the equator

the mean-state SST shifts from cooling to warming in the eastern equatorial Pacific.

The sign of SST change induced by chlorophyll effect can be explained by two mechanisms (Fig. 12): (1) the warming effect mainly stems from the direct heating induced by chlorophyll within the mixed layer and subsurface warming; (2) the cooling effect can be attributed to indirect cooling induced by the adjustment of ocean circulation and enhanced vertical mixing (Fig. 12a). As shown in this study, the net effect of the direct heating and indirect cooling acts to determine the SST cooling or warming in the eastern equatorial Pacific; i.e., the relatively dominant roles of thermodynamic process or dynamic process (Fig. 12). With the increase in α (coupling intensity), the initial warming induced by chlorophyll tends to induce anomalous westerly winds in the eastern equatorial Pacific. The anomalous westerly winds act to suppress the Ekman divergence in the eastern equatorial Pacific and further weakens the dynamical cooling effect. Meanwhile, the latent heat flux is reduced due to a decrease in wind speed (Fig. 12b). Therefore, the chlorophyll-induced direct warming and indirect cooling both weaken, but the weakened amplitude of direct warming due to the changes in net surface heat flux is relatively small compared to the change in indirect cooling, consequently leading to a net warming effect in the eastern tropical Pacific (Fig. 12b).

Except for previously identified direct heating and indirect cooling mechanisms, we found remarkable differences in the meridional SST responses induced by chlorophyll effects in this modeling results (Fig. 12). In the off-equatorial central Pacific, a persistent cooling condition north of the equator and a warming condition south of the equator act to induce cross-equatorial northerly winds due to the WES mechanism. This cross-equatorial northerly wind shifts eastward and further weakens the trade winds; the decrease in wind speed suppresses the LHF feedback and further leads to an increase in SST south of the equator (Fig. 12b). When taking $\alpha > 1.0$, the zonal SST difference induced by the presence of chlorophyll are gradually increased, leading to an intensified Bjerknes feedback along the equator. Meanwhile, chlorophyll-induced WES feedback intensifies under the weak coupling condition and maintains SST warming in the southern subtropical Pacific under strong coupling condition. This warming is also seen in the recent GFDL-CM2.1 simulations (e.g., Lim et al. 2018), indicating the potential chlorophyll effect from the southern subtropical Pacific on the equatorial Pacific should be investigated in the future.

4.2 Discussion

As demonstrated, the chlorophyll-induced SST change can be further modulated by coupled ocean–atmosphere interaction, which not only involves the zonal direction, but also the meridional direction, acting to determine the SST condition (cooling or warming) under different coupling intensity. As shown in Guilyardi (2006), inter-model differences in coupling intensity exist widely in the CMIP models. The ocean–atmosphere coupling intensity (Bjerknes feedback) is often computed as the regression of Niño4 wind stress over Niño3 SST (10^{-3} N m^{-2} °C^{-1}) as illustrated in Bellenger et al. (2014). Using this method, the coupling intensity is about 12×10^{-3} N m^{-2} °C^{-1} in the present-day climate. However, in the CMIP5 historical simulations, most climate models underestimate the coupling intensity from 2 to 10×10^{-3} N m^{-2} °C^{-1}. Therefore, the underestimation of coupling intensity in the current climate models may further exert a pronounced influence on the chlorophyll-induced heating effect. For instance, as shown in Park et al. (2014a) using the GFDL-CM2.1 simulation, the presence of chlorophyll tends to induce a cooling effect under the uncoupled and coupled condition. Actually, the coupling intensity in GFDL-CM2.1 is weaker than the observation as illustrated in Fig. 7 by Bellenger et al. (2014). Meanwhile, as shown in this study, chlorophyll tends to induce a cooling effect on the eastern equatorial Pacific under the weakly coupled condition ($\alpha < 1.01$). Thus, the chlorophyll-induced SST change may manifest diverse patterns (an SST warming or cooling) associated with varying coupling intensity. It is noted that the effects of chlorophyll in other basins (e.g., the Atlantic Ocean and the Indian Ocean) and the subtropical region have been considered by Park et al. (2014b), which may further affect the tropical Pacific climate through the atmosphere bridge, but has not been taken into account in our models.

In the Coupled Model Intercomparison Project phase 5 and 6 (CMIP5/6), more ESMs with explicitly represented biogeochemical processes have been introduced to project the future climate change, and the way how interactions between physical and ocean biological processes tend to affect SST is not known (Séférian et al. 2020). Therefore, the related evaluation of bio-physical feedback should be addressed carefully.

Due to the pronounced effect of chlorophyll on the mean state SST, its related effects on the tropical climate from the decade timescale to long-term trends need to be examined in the future. Previous studies showed that global mean chlorophyll concentration tends to be decreased in the twentieth century (Boyce et al. 2010, 2014; McQuatters-Gollop et al. 2011). Because the decrease in chlorophyll acts to induce more solar radiation penetrating out of the ML and entering the deeper subsurface ocean, the heat may be advected to the equatorial ocean through the subtropical cells after several decades and further affect tropical Pacific climate variability, giving rise to the ENSO modulations (Gnanadesikan and Anderson 2009). It is noted that the presence of chlorophyll tends to affect interdecadal variability of SST in some cases

(e.g., $\alpha = 1.15$ or 1.05; figure not shown), which needs to be investigated in the future.

The current study indicates several important caveats. The coupled model tends to overestimate the concentration of chlorophyll near the equator compared with satellite observation (the bias≈0.1 mg m^{-3}). Lim et al. (2018) found that the overestimated chlorophyll in the model acts to increase the cold SST bias in the Cold Tongue of the tropical Pacific; after correcting the chlorophyll bias, the SST cold bias tends to be largely removed in the GFDL model. Therefore, the model bias in the chlorophyll simulation should be taken into account for this study; such model bias may be further amplified through atmospheric feedback. In addition, the model we adopted is a simplified regional coupled model without considering the remote inter-basin effect from the Indian and the Atlantic Ocean, or the subtropical Pacific (Patara et al. 2012; Park et al. 2014a). Therefore, the chlorophyll effect on the tropical Pacific is not allowed to influence the subtropical Pacific or other basins, which in turn can further affect the tropical Pacific mean state itself; this process needs to be investigated in the future. Additionally, the effect from other scatter matters like color dissolved organic matters (CDOM) on the ocean has been considered into the ESM, and modelling results show that CDOM exhibits a significant impact on the global warming hiatus and extreme weather (Kim et al. 2018; Gnanadesikan et al. 2019). Therefore, the related effects of CDOM on the tropical Pacific climate should be considered in combination with chlorophyll in the future.

Acknowledgements The authors wish to thank the anonymous reviewers for their insightful comments that greatly helped to improve the original manuscript. The author would like to thank Dr. Lei Zhou for his comments. This research was supported by the National Natural Science Foundation of China (NFSC; Grant nos. 42006001, 42030410), the Strategic Priority Research Program of the Chinese Academy of Sciences (Grant no. XDB42000000 (XDB42040100, XDB42040103), XDB 40000000, XDA19060102), the National Key Research and Development Program of China (2017YFC1404102 (2017YFC1404100)), the NSFC-Shandong Joint Fund for Marine Science Research Centers (U1406402), China Postdoctoral Science Foundation (2019M662453) and Qingdao postdoctoral application research project.

References

Anderson WG, Gnanadesikan A, Hallberg R et al (2007) Impact of ocean color on the maintenance of the Pacific Cold Tongue. Geophys Res Lett 34:1–5. https://doi.org/10.1029/2007GL030100

Anderson W, Gnanadesikan A, Wittenberg A (2009) Regional impacts of ocean color on tropical Pacific variability. Ocean Sci 5:313–327. https://doi.org/10.5194/os-5-313-2009

Ballabrera-Poy J, Murtugudde R, Zhang R-H, Busalacchi AJ (2007) Coupled ocean-atmosphere response to seasonal modulation of ocean color: impact on interannual climate simulations in the tropical pacific. J Clim 20:353–374. https://doi.org/10.1175/JCLI3958.1

Bellenger H, Guilyardi E, Leloup J et al (2014) ENSO representation in climate models: from CMIP3 to CMIP5. Clim Dyn 42:1999–2018. https://doi.org/10.1007/s00382-013-1783-z

Bjerknes J (1969) Atmospheric teleconnections from the equatorial pacific. Mon Weather Rev 97:163–172. https://doi.org/10.1175/1520-0493(1969)097%3c0163:ATFTEP%3e2.3.CO;2

Boyce DG, Lewis MR, Worm B (2010) Global phytoplankton decline over the past century. Nature 466:591–596. https://doi.org/10.1038/nature09268

Boyce DG, Dowd M, Lewis MR, Worm B (2014) Estimating global chlorophyll changes over the past century. Prog Oceanogr 122:163–173. https://doi.org/10.1016/j.pocean.2014.01.004

Boyer TP, Garcia HE, Locarnini RA et al (2018) World Ocean Atlas 2018

Chang P (1996) The role of the dynamic ocean-atmosphere interactions in tropical seasonal cycle. J Clim 9:2973–2985. https://doi.org/10.1175/1520-0442(1996)009%3c2973:TROTDO%3e2.0.CO;2

Chang P, Ji L, Saravanan R (2001) A hybrid coupled model study of tropical atlantic variability. J Clim 14:361–390. https://doi.org/10.1175/1520-0442(2001)013%3c0361:AHCMSO%3e2.0.CO;2

Chen D, Rothstein LM, Busalacchi AJ (1994) A HYBRID VERTICAL MIXING SCHEME AND ITS APPLICATION TO TROPICAL OCEAN MODELS. J Phys Oceanogr 24:2156–2179. https://doi.org/10.1175/1520-0485(1994)024%3c2156:AHVMSA%3e2.0.CO;2

Christian JR, Verschell MA, Murtugudde R et al (2001) Biogeochemical modelling of the tropical Pacific Ocean. I: seasonal and interannual variability. Deep Sea Res Part II Top Stud Oceanogr 49:509–543. https://doi.org/10.1016/S0967-0645(01)00110-2

England MH, McGregor S, Spence P et al (2014) Recent intensification of wind-driven circulation in the Pacific and the ongoing warming hiatus. Nat Clim Chang 4:222–227. https://doi.org/10.1038/nclimate2106

Forget G, Ferreira D (2019) Global ocean heat transport dominated by heat export from the tropical Pacific. Nat Geosci 12:351–354. https://doi.org/10.1038/s41561-019-0333-7

Gao C, Zhang R-H (2017) The roles of atmospheric wind and entrained water temperature (Te) in the second-year cooling of the 2010–12 La Niña event. Clim Dyn 48:597–617. https://doi.org/10.1007/s00382-016-3097-4

Gent PR, Cane MA (1989) A reduced gravity, primitive equation model of the upper equatorial ocean. J Comput Phys 81:444–480. https://doi.org/10.1016/0021-9991(89)90216-7

Gildor H (2003) A role for ocean biota in tropical intraseasonal atmospheric variability. Geophys Res Lett 30:1460. https://doi.org/10.1029/2002GL016759

Gill AE (1980) Some simple solutions for heat-induced tropical circulation. Q J R Meteorol Soc 106:447–462. https://doi.org/10.1002/qj.49710644905

Gnanadesikan A, Anderson WG (2009) Ocean water clarity and the ocean general circulation in a coupled climate model. J Phys Oceanogr 39:314–332. https://doi.org/10.1175/2008JPO3935.1

Gnanadesikan A, Kim GE, Pradal MS (2019) Impact of colored dissolved materials on the annual cycle of sea surface temperature: potential implications for extreme ocean temperatures. Geophys Res Lett 46:861–869. https://doi.org/10.1029/2018GL080695

Graham T (2014) The importance of eddy permitting model resolution for simulation of the heat budget of tropical instability waves. Ocean Model 79:21–32. https://doi.org/10.1016/j.ocemod.2014.04.005

Guilyardi E (2006) El Niño–mean state–seasonal cycle interactions in a multi-model ensemble. Clim Dyn 26:329–348. https://doi.org/10.1007/s00382-005-0084-6

Haney RL (1971) Surface thermal boundary condition for ocean circulation models. J Phys Oceanogr 1:241–248

Jochum M, Cronin MF, Kessler WS, Shea D (2007) Observed horizontal temperature advection by tropical instability waves. Geophys Res Lett 34:20–23. https://doi.org/10.1029/2007GL029416

Jochum M, Yeager S, Lindsay K et al (2010) Quantification of the feedback between phytoplankton and ENSO in the community climate system model. J Clim 23:2916–2925. https://doi.org/10.1175/2010JCLI3254.1

Karnauskas KB, Murtugudde R, Busalacchi AJ (2007) The effect of the Galápagos Islands on the equatorial Pacific cold tongue. J Phys Oceanogr 37:1266–1281. https://doi.org/10.1175/JPO3048.1

Kim GE, Gnanadesikan A, Del Castillo CE, Pradal MA (2018) Upper ocean cooling in a coupled climate model due to light attenuation by yellowing materials. Geophys Res Lett 45:6134–6140. https://doi.org/10.1029/2018GL077297

Kosaka Y, Xie S-PP (2013) Recent global-warming hiatus tied to equatorial Pacific surface cooling. Nature 501:403–407. https://doi.org/10.1038/nature12534

Kraus EB, Turner JS (1967) A one-dimensional model of the seasonal thermocline II. The general theory and its consequences. Tellus 19:98–106. https://doi.org/10.3402/tellusa.v19i1.9753

Lengaigne M, Menkes C, Aumont O et al (2007) Influence of the oceanic biology on the tropical Pacific climate in a coupled general circulation model. Clim Dyn 28:503–516. https://doi.org/10.1007/s00382-006-0200-2

Lewis MR, Carr M-E, Feldman GC et al (1990) Influence of penetrating solar radiation on the heat budget of the equatorial Pacific Ocean. Nature 347:543–545. https://doi.org/10.1038/347543a0

Li G, Xie S-P, Du Y, Luo Y (2016) Effects of excessive equatorial cold tongue bias on the projections of tropical Pacific climate change. Part I: the warming pattern in CMIP5 multi-model ensemble. Clim Dyn 47:3817–3831. https://doi.org/10.1007/s00382-016-3043-5

Liang X, Wu L (2013) Effects of solar penetration on the annual cycle of sea surface temperature in the North Pacific. J Geophys Res Ocean 118:2793–2801. https://doi.org/10.1002/jgrc.20208

Lim HG, Park JY, Kug JS (2018) Impact of chlorophyll bias on the tropical Pacific mean climate in an earth system model. Clim Dyn 51:2681–2694. https://doi.org/10.1007/s00382-017-4036-8

Lin P, Liu H, Zhang X (2007) Sensitivity of the upper ocean temperature and circulation in the equatorial Pacific to solar radiation penetration due to phytoplankton. Adv Atmos Sci 24:765–780. https://doi.org/10.1007/s00376-007-0765-7

Lin P, Liu H, Zhang X (2008) Effect of chlorophyll-a spatial distribution on upper ocean temperature in the central and eastern equatorial Pacific. Adv Atmos Sci 25:585–596. https://doi.org/10.1007/s00376-008-0585-4

Lin P, Liu H, Yu Y, Zhang X (2011) Response of sea surface temperature to chlorophyll-a concentration in the tropical Pacific: annual mean, seasonal cycle, and interannual variability. Adv Atmos Sci 28:492–510. https://doi.org/10.1007/s00376-010-0015-2

Löptien U, Eden C, Timmermann A et al (2009) Effects of biologically induced differential heating in an eddy-permitting coupled ocean-ecosystem model. J Geophys Res 114:C06011. https://doi.org/10.1029/2008JC004936

Luo J-J, Masson S, Roeckner E et al (2005) Reducing climatology bias in an ocean-atmosphere CGCM with improved coupling physics. J Clim 18:2344–2360. https://doi.org/10.1175/JCLI3404.1

Maritorena S, d'Andon OHF, Mangin A, Siegel DA (2010) Merged satellite ocean color data products using a bio-optical model: characteristics, benefits and issues. Remote Sens Environ 114:1791–1804. https://doi.org/10.1016/j.rse.2010.04.002

Marzeion B, Timmermann A, Murtugudde R, Jin F-FF (2005) Biophysical feedbacks in the tropical Pacific. J Clim 18:58–70. https://doi.org/10.1175/JCLI3261.1

McQuatters-Gollop A, Reid PC, Edwards M et al (2011) Is there a decline in marine phytoplankton? Nature 472:591–596. https://doi.org/10.1038/nature09950

Morel A, Antoine D (1994) Heating rate within the upper ocean in relation to its bio–optical state. J Phys Oceanogr 24:1652–1665. https://doi.org/10.1175/1520-0485(1994)024%3c1652:HRWTUO%3e2.0.CO;2

Murtugudde R, Seager R, Busalacchi A (1996) Simulation of the tropical oceans with an ocean GCM coupled to an atmospheric mixed-layer model. J Clim 9:1795–1815. https://doi.org/10.1175/1520-0442(1996)009%3c1795:SOTTOW%3e2.0.CO;2

Murtugudde R, Beauchamp J, McClain CR et al (2002) Effects of penetrative radiation of the upper tropical ocean circulation. J Clim 15:470–486. https://doi.org/10.1175/1520-0442(2002)015%3c0470:EOPROT%3e2.0.CO;2

Nakamoto S, Kumar SP, Oberhuber JM et al (2001) Response of the equatorial Pacific to chlorophyll pigment in a mixed layer isopycnal ocean general circulation model. Geophys Res Lett 28:2021–2024. https://doi.org/10.1029/2000GL012494

Ohlmann JC, Siegel DA, Mobley CD (2000) Ocean radiant heating. Part I: optical influences. J Phys Oceanogr 30:1833–1848. https://doi.org/10.1175/1520-0485(2000)030%3c1833:ORHPIO%3e2.0.CO;2

Park J-Y, Kug J-S, Seo H, Bader J (2014a) Impact of bio-physical feedbacks on the tropical climate in coupled and uncoupled GCMs. Clim Dyn 43:1811–1827. https://doi.org/10.1007/s00382-013-2009-0

Park J-Y, Kug JS, Park YG (2014b) An exploratory modeling study on bio-physical processes associated with ENSO. Prog Oceanogr 124:28–41. https://doi.org/10.1016/j.pocean.2014.03.013

Patara L, Vichi M, Masina S et al (2012) Global response to solar radiation absorbed by phytoplankton in a coupled climate model. Clim Dyn 39:1951–1968. https://doi.org/10.1007/s00382-012-1300-9

Paulson C, Simpson J (1977) Irradiance measurements in the upper ocean. J Phys Oceanogr 7:952–956. https://doi.org/10.1175/1520-0485(1977)007%3c0952:IMITUO%3e2.0.CO;2

Price JF, Weller RA, Pinkel R (1986) Diurnal Cycling: observations and models of the upper ocean response to diurnal heating, cooling, and wind mixing. J Geophys Res 91:8411–8427. https://doi.org/10.1029/jc091ic07p08411

Schneider EK, Zhu Z (1998) Sensitivity of the simulated annual cycle of sea surface temperature in the equatorial Pacific to sunlight penetration. J Clim 11:1932–1950. https://doi.org/10.1175/1520-0442-11.8.1932

Seager R, Blumenthal MB, Kushnir Y (1995) An advective atmospheric mixed layer model for ocean modeling purposes: global simulation of surface heat fluxes. J Clim 8:1951–1964. https://doi.org/10.1175/1520-0442(1995)008%3c1951:AAAMLM%3e2.0.CO;2

Seager R, Cane M, Henderson N et al (2019) Strengthening tropical Pacific zonal sea surface temperature gradient consistent with rising greenhouse gases. Nat Clim Chang 9:517–522. https://doi.org/10.1038/s41558-019-0505-x

Séférian R, Berthet S, Yool A et al (2020) Tracking improvement in simulated marine biogeochemistry between CMIP5 and CMIP6. Curr Clim Chang Reports 6:95–119. https://doi.org/10.1007/s40641-020-00160-0

Shell KM (2003) Atmospheric response to solar radiation absorbed by phytoplankton. J Geophys Res 108:1–8. https://doi.org/10.1029/2003JD003440

Siegel DA, Ohlmann JC, Washburn L et al (1995) Solar radiation, phytoplankton pigments and the radiant heating of the

equatorial Pacific warm pool. J Geophys Res 100:4885. https://doi.org/10.1029/94JC03128
Sweeney C, Gnanadesikan A, Griffies SM et al (2005) Impacts of shortwave penetration depth on large-scale ocean circulation and heat transport. J Phys Oceanogr 35:1103–1119. https://doi.org/10.1175/JPO2740.1
Syu H-H, Neelin JD, Gutzler D (1995) Seasonal and interannual variablity in hybrid coupled GCM. J Clim 8:2121–2143
Tian F, Zhang R-H, Wang X (2018) A coupled ocean physics-biology modeling study on tropical instability wave-induced chlorophyll impacts in the Pacific. J Geophys Res Ocean 123:5160–5179. https://doi.org/10.1029/2018JC013992
Tian F, Zhang R-H, Wang X (2019) A positive feedback onto ENSO due to tropical instability wave (TIW)-induced chlorophyll effects in the Pacific. Geophys Res Lett 46:889–897. https://doi.org/10.1029/2018GL081275
Wang XJ, Le Borgne R, Murtugudde R et al (2008) Spatial and temporal variations in dissolved and particulate organic nitrogen in the equatorial Pacific: biological and physical influences. Biogeosciences 5:1705–1721. https://doi.org/10.5194/bg-5-1705-2008
Wang X, Le Borgne R, Murtugudde R et al (2009a) Spatial and temporal variability of the phytoplankton carbon to chlorophyll ratio in the equatorial Pacific: a basin-scale modeling study. J Geophys Res 114:C07008. https://doi.org/10.1029/2008JC004942
Wang XJ, Behrenfeld M, Le Borgne R et al (2009b) Regulation of phytoplankton carbon to chlorophyll ratio by light, nutrients and temperature in the equatorial pacific ocean: a basin-scale model. Biogeosciences 6:391–404. https://doi.org/10.5194/bg-6-391-2009
Wang C, Zhang L, Lee SS-K et al (2014) A global perspective on CMIP5 climate model biases. Nat Clim Chang 4:201–205. https://doi.org/10.1038/nclimate2118
Wetzel P, Maier-Reimer E, Botzet M et al (2006) Effects of ocean biology on the penetrative radiation in a coupled climate model. J Clim 19:3973–3987. https://doi.org/10.1175/JCLI3828.1
Xie S-P (1994) On the genesis of the equatorial annual cycle. J Clim 7:2008–2013. https://doi.org/10.1175/1520-0442(1994)007%3c2008:OTGOTE%3e2.0.CO;2
Xie S-P, Philander SGH (1994) A coupled ocean-atmosphere model of relevance to the ITCZ in the eastern Pacific. Tellus A Dyn Meteorol Oceanogr 46:340–350. https://doi.org/10.3402/tellusa.v46i4.15484
Zhang R-H (2015) Structure and effect of ocean biology-induced heating (OBH) in the tropical Pacific, diagnosed from a hybrid coupled model simulation. Clim Dyn 44:695–715. https://doi.org/10.1007/s00382-014-2231-4
Zhang R-H, Busalacchi AJ (2009) An empirical model for surface wind stress response to SST forcing induced by tropical instability waves (TIWs) in the Eastern Equatorial Pacific. Mon Weather Rev 137:2021–2046. https://doi.org/10.1175/2008MWR2712.1
Zhang R-H, Kleeman R, Zebiak SE et al (2005) An empirical parameterization of subsurface entrainment temperature for improved SST anomaly simulations in an intermediate ocean model. J Clim 18:350–371. https://doi.org/10.1175/JCLI-3271.1
Zhang R-H, Busalacchi AJ, Wang X et al (2009) Role of ocean biology-induced climate feedback in the modulation of El Niño-Southern Oscillation. Geophys Res Lett 2009:36. https://doi.org/10.1029/2008GL036568
Zhang R-H, Zheng F, Zhu J, Wang Z (2013) A successful real-time forecast of the 2010–11 La Niña event. Sci Rep 3:1108. https://doi.org/10.1038/srep01108
Zhang R-H, Tian F, Wang X (2018a) A new hybrid coupled model of atmosphere, ocean physics, and ocean biogeochemistry to represent biogeophysical feedback effects in the tropical Pacific. J Adv Model Earth Syst 10:1901–1923. https://doi.org/10.1029/2017MS001250
Zhang R-H, Tian F, Wang X (2018b) Ocean chlorophyll-induced heating feedbacks on ENSO in a coupled ocean physics-biology model forced by prescribed wind anomalies. J Clim 31:1811–1832. https://doi.org/10.1175/JCLI-D-17-0505.1
Zhang R-H, Tian F, Busalacchi AJ, Wang X (2019a) Freshwater flux and ocean chlorophyll produce nonlinear feedbacks in the tropical Pacific. J Clim 32:2037–2055. https://doi.org/10.1175/JCLI-D-18-0430.1
Zhang R-H, Tian F, Zhi H, Kang X (2019b) Observed structural relationships between ocean chlorophyll variability and its heating effects on the ENSO. Clim Dyn 53:5165–5186. https://doi.org/10.1007/s00382-019-04844-8
Zhang R-H, Yu Y, Song Z et al (2020) A review of progress in coupled ocean-atmosphere model developments for ENSO studies in China. J Oceanol Limnol 38:930–961. https://doi.org/10.1007/s00343-020-0157-8
Zhu Y, Zhang R-H (2018) An argo-derived background diffusivity parameterization for improved ocean simulations in the tropical Pacific. Geophys Res Lett 45:1509–1517. https://doi.org/10.1002/2017GL076269
Zhu Y, Zhang R-H (2019) A modified vertical mixing parameterization for its improved ocean and coupled simulations in the tropical Pacific. J Phys Oceanogr 49:21–37. https://doi.org/10.1175/JPO-D-18-0100.1
Zhu Y, Zhang R-H, Sun J (2020) North Pacific upper-ocean cold temperature biases in CMIP6 simulations and the role of regional vertical mixing. J Clim. https://doi.org/10.1175/JCLI-D-19-0654.1